# Using time-delayed mutual information to discover and interpret temporal correlation structure in complex populations

D. J. Albers[1, *] and George Hripcsak[1, †]

[1] *Department of Biomedical Informatics, Columbia University,*
*622 West 168th Street, VC-5, New York, NY 10032*

(Dated: October 20, 2011)

This paper addresses how to calculate and interpret the time-delayed mutual information for a complex, diversely and sparsely measured, possibly non-stationary *population* of time-series of unknown composition and origin. The primary vehicle used for this analysis is a comparison between the time-delayed mutual information *averaged* over the population and the time-delayed mutual information of an aggregated population (here aggregation implies the population is conjoined before any statistical estimates are implemented). Through the use of information theoretic tools, a sequence of practically implementable calculations are detailed that allow for the average and aggregate time-delayed mutual information to be interpreted. Moreover, these calculations can be also be used to understand the degree of homo- or heterogeneity present in the population. To demonstrate that the proposed methods can be used in nearly any situation, the methods are applied and demonstrated on the time series of glucose measurements from two different subpopulations of individuals from the Columbia University Medical Center electronic health record repository, revealing a picture of the composition of the population as well as physiological features.

PACS numbers:
Keywords:

*In this paper we show how to apply time-delayed mutual information to a sparse, irregularly measured, complicated population of time-dependent data. At a fundamental level, the technical problem is a probability density function (PDF) estimation problem; specifically, one can* average *PDF estimates* or *one can aggregate the data set* before *estimating the PDF. To understand and interpret these two means of coping with a population of time-series, one must address four issues: (i) estimator bias; (ii) normalization, or distribution support-based effects; (iii) deviations from the single source case for average and aggregate; and (iv) practical interpretation. Scientifically, this paper works to develop an infrastructure, and demonstrates how to use it, by studying the time-dependent correlation structure in physiological variables of humans — in a population of glucose time-series. In the end, we not only provide a practically actionable set of information theoretic computations that yield insight into the population composition* and *the time-dependent correlation structure, but we also detail the time-dependent correlation structure and the degree of homogeneity within a broad population of humans via their glucose measurements.*

## I. INTRODUCTION

It is no surprise that aggregating collections of elements or data streams can allow for a productive analysis and understanding of the individual elements that make up the aggregated population. In fact, the aggregation of many elements into a measurable population can be pivotal in providing a means to study systems where the individual elements are difficult, expensive, or dangerous to measure. (Note that by aggregation, we mean combining *sets* of measurements in such a way that they can be treated as a single *set* of measurements that can be analyzed.) That aggregation provides a basis for analysis lies in the fact that the application of most statistical methods, such as statistical averages, probability density estimates, and techniques based on such fundamental methods (i.e., information theory, ergodic theory, etc.), require large numbers of data points. While some fields have gained much from the analysis of aggregated populations of elements — such as advances made in the physical sciences with the advent of statistical mechanics — many fields have not been so fortunate. A primary source of difficulty with aggregation in these less fortunate contexts lies in the fact that fortune or ruin often depends on the ability to aggregate measured elements such that statistical averages can be taken. Usually this means one must have a population of elements whose statistical properties being quantified are drawn from the same distributions. This requirement presents two inextricable problems, verifying that a population is homogeneous enough to produce representative statistics when aggregated, and determining whether a statistical analysis technique will yield the same outcome for the average over the population and for the aggregated population.

[*] Electronic address: david.albers@dbmi.columbia.edu
[†] Electronic address: hripcsak@columbia.edu

With these broad issues in mind, here we focus on applying time-delayed mutual information to a population in an attempt to understand *the time-dependent nonlinear correlation between measurements, or the degree of predictability of measurements for members of a population.* We wish to apply this, however, to a system whose members may: (i) have differing numbers of measurements; (ii) have too few measurements for probability densities (or any other statistical quantities) to be estimated; (iii) be non-stationary; (iv) have very diverse underlying probability distributions or statistical states; and (v) may be measured in a highly irregular manner in time. In short, this paper details how to apply and interpret information theoretic analysis to a diversely measured, possibly statistically diverse population that needs to be aggregated for the information theoretic quantities to be calculable. Thus, this paper complements and contrasts with the research such as is presented in Ref. [1] where dynamical reconstruction of a uniformly measured stationary systems with short time-series are the focus. The particular population we focus on in this paper is a subpopulation of human beings who received care at the Columbia University Medical Center (CUMC). The particular time-series we are focusing on are clinical chemistry measurements (measurements such as glucose, that detail physiological functioning of humans) for this population. Nevertheless, it is important to note that the analysis presented is not limited to any particular population of measurements.

### A. A reader's guide: the outline of this paper

Broadly this paper can be split into two main components. The first component is primarily theoretical and includes: a background section (III); a section about TDMI-specific estimator bias (IV); a section focusing on how the TDMI for a population can deviate from the TDMI of an individual stationary source (V); and finally a section explaining how to use the TDMI population calculations to characterize diversity in a population (VI). Second, following the more theoretical sections, are the computational sections including: a section explaining how to use the TDMI population calculations to characterize diversity in a population (VI); a section proposing some non-TDMI based metrics for evaluating population diversity that help verify the TDMI-based methods (VII); a section summarizing the TDMI methodology explicitly (VIII); and finally the data-based section IX demonstrating the methodology. Regardless of intent, readers will need the to read the introduction sections I-III and the summary.

## II. MOTIVATING EXAMPLES

The theory-based motivation for this work is to devise a way to calculate and interpret the time-delayed mutual information (TDMI) [2] [3] in the context of a *population* of time-series that are both sampled irregularly and are from (possibly) statistically distinct sources. More concretely, the motivation for this work comes from the desire to understand human health dynamics (i.e., physiology, complex phenotype definitions such as diseases, basic biology, etc) based on the constrains of real data present in the electronic health record (EHR) repository at Columbia University Medical Center (CUMC) (note, CUMC is affiliated with NewYork-Presbyterian Hospital). These data represents all the information that doctors at CUMC collect; the CUMC EHR is one of the oldest and most complete EHRs in the country, and thus represents the type of data that future EHRs will likely contain. EHR data are of note because EHRs contain most of the *macroscopic*, biologically based, data on humans in existence.

For instance, the CUMC EHR contains information regarding 2.5 million patients over 20 years and contains graphical images, laboratory data, drug data, doctor and nurse notes, billing data, and demographic data, most of which is highly dependent on time; moreover, the *amount* of data is growing exponentially. Despite the quantity of data, EHR data can be difficult to use; in particular, EHR data is characterized by: diverse irregular sampling, measurements correlated to statistical state, nonstationarity, statistically diverse population, very large populations with few measurements, and very diverse data types. Nevertheless, if these data prove to be useful for understanding human dynamics, a subject that is not completely without controversy [4] [5] [6], it may be possible: to define complex diseases and other phenotypes (based on real, population scale data); to understand how disease and treatment of disease evolve in complex and interconnected ways [7] [8]; to define completeness of medical records; correlate drugs to side effects and benefits; to monitor population-wide disease spread and evolution; and to carry out many other practical applications that can be gained from understanding population-wide human health and biology. The approach upon which this work is based represents a radical departure from the standard utilization of biomedical data; here the data are studied using nonlinear physics methodology and has been termed by some [9] as the physics of living things.

Of course, another advantage of motivating the work in this paper with a data set with complex properties is that it allows for the generalization of the results to many other contexts whose data have a subset of the complexities. Outside of laboratory science, nearly all data sets are difficult to control and have many of the same problems that EHR data have. Thus, we claim that while we apply our analysis in the context of human health and physiology, our methods can be easily generalized to nearly all time-dependent contexts; e.g., astronomy [10], geology [11], climatology [12], and genetics [13].

## III. INFORMATION THEORY BACKGROUND

Begin with time-series, $X = (x_1(t_1), \cdots, x_N(t_N))$ of real numbers. Next, denote all of the *pairs* of points in $X$ separated by a either index time, $\tau = i - j$ (where $i > j$ are the indices of $t_i$ and $t_j$ respectively), or real time, $\delta t = t_i - t_j$ (again assume $t_i > t_j$), by $X[\tau]$ or $X[\delta t]$ respectively. Note that $\tau$ is always an integer while $\delta t$ can take continuous real values. For this section we will limit the discussion to $X[\tau]$, but note that the $X[\delta t]$ case follows identically. Note that in this circumstance, $X[\tau]$ can be used to approximate a *joint* (two-dimensional) PDF; further, note that the marginal distributions of $X[\tau]$ are approximated by $X[\tau](1) = X(i)$ and $X[\tau](2) = X(i-\tau)$ respectively.

To estimate either the information entropy, or the TDMI for this time-series [3] [2], one must first estimate various probability density functions (PDF) [14]. In order to specify a PDF, one needs to both specify the support of the PDF, $S$, and the PDF itself, $p(X)$. Moreover, intuitively, the support of the PDF is the interval over which the $x_i$'s lie, or, the support of the PDF of $X$ is $S = [\min(X), \max(X)]$. However, when *estimating* a PDF from data, the support will always be collected in a series of bins; thus, there also exists an *abstract support*, $\mathcal{S}$, which consists of the *explicit* bins of the data used to estimate the PDF *disconnected from the values the bins are assigned externally.* Thus $\mathcal{S}$ does not explicitly represent numbers in $X$; while this may seem like a strange point to make, the difference between $S$ and $\mathcal{S}$ will be critical later in this paper. Finally, note, we will always assume that PDFs in this paper have *compact support* [15].

Now, given the random variable $X$ and its associated PDF, $p(X)$, the information entropy of a time series generated by $X$ is defined by:

$$h_I = -\int_S p(X) \log(p(X)) dx. \quad (1)$$

Similarly, the TDMI is defined by:

$$\begin{aligned} &I(X(i); X(i-\tau)) = \\ &I(X[\tau]) = \quad (2) \\ &\int p(X(i), X(i-\tau)) \log \frac{p(X(i), X(i-\tau))}{p(X(i))p(X(i-\tau))} dX(i) dX(i-\tau) \end{aligned}$$

Thus the TDMI can be thought of as an auto-information measure that depends on a delay (e.g., $\tau$ or $\delta t$).

Given this infrastructure, fundamentally there are two ways of conjoining a population: (i) averaging the TDMI for each member of the population; and (ii) aggregating the population *before* the PDFs are estimated *without* intermixing the members of the population. As we will see, in the context of a heterogeneous population, these two approaches will yield both differing numerical results and differing interpretations.

Computationally it is important to note that we will employ both a KDE estimator [16] [17] [18] and a standard histogram estimator for all PDF calculations. We explicitly use the estimator developed in Ref. [16] with a Gaussian kernel and a bandwidth of 100; the histogram estimator is of our own design and has a bandwidth of 20. The results detailed in this paper are relatively insensitive to these parameter settings (e.g., a 10% change in the bandwidth will not produce a qualitatively different result). Moreover, in this paper we will estimate the bias using the fixed point bias estimation technique [19], which amounts to various random permutations of temporal ordering of the time-series used to generate the PDFs and will be introduced in more detail in section IV B. Finally, while this paper only addresses the continuous case, the discrete case follows more or less identically with integrals replaced by sums.

### A. Average TDMI

To formulate the average TDMI for a population, we begin by arguing that the average mutual information of a vector of individuals (a population) is the same as the average of the mutual informations of each individual, if the individuals are independent. These cases represent conjoining a population *after the PDFs have been estimated*; in essence we are just arguing that taking an average before or after the TDMI integration is performed does not affect the resultant TDMI.

Assume all processes are stationary. Define a vector-valued process $X$, where $X(t) = [X_1(t), X_2(t), \cdots, X_N(t)]$; this leads to a the following definition of multivariate mutual information:

$$\begin{aligned} &I[X(t); X(t+j)] = \\ &\int p(X(t), X(t+j)) \quad (3) \\ &\log \frac{p(X(t), X(t+j))}{p(X(t))p(X(t+j))} dX(t) dX(t+j) \end{aligned}$$

noting that $p(\cdot)$ is the probability density associated with the given random variable, and $X(\cdot)$ and $dX(\cdot)$ are both vectors. We want the following statement to be true:

$$\frac{1}{N} I[X(t); X(t+j)] = \frac{1}{N} \sum_{i=1}^{N} I[X_i(t); X_i(t+j)] \quad (4)$$

We claim that the *sufficient* condition for 4 to hold is for the $X_i$ processes to be non-interacting, or statistically independent. It is important to note that it is *not* necessary that the $X_i$'s be non-interacting copies of the *same process* — the processes only have to be statistically independent. It is not too difficult to verify our claim algebraically, one merely applies the chain rule for mutual information to Eq. 4; moreover, conceptually understanding why our claim is correct is rather straightforward. Begin by noting that if the $X_i$'s are independent, they form an orthogonal set of probability densities, or a product measure on $N$-dimensional Euclidean space. Thus the integral of each variable will be independent of the others simply because the variables are orthogonal and thus not functions of one another (c.f., Fubini's theorem [20]).

The conclusion is that, the average TDMI for the population is simply the *canonically calcuated* TDMI for the individuals of the population, averaged.

### B. Aggregate TDMI

To understand the construction where the population is aggregated *before* the PDFs are estimated, assume, as we did in section III A, a stationary, vector-valued process $X$, where $X(t) = [X_1(t), X_2(t), ...X_N(t)]$, where $N$ denotes the number of individuals in the population. Next, assume that each element emits a time-series of length $n_i$; without loss of generality, in this section assume that $n_i = n$.

Aggregating the population into a time-series for which the PDFs can be estimated can be done in one of two ways. The first method involves concatenating the entire set of time-series into one scalar time-series of length $Nn$ and then treating this concatenated time-series like a time-series from a single source; denote this aggregation method as *inter-source aggregation.* We will *not* study this as this calculation needlessly adds noise via the *intermixing of elements* and is hard to rectify with mathematics. The second method, denoted the *intra-source aggregation* because sources are not intermixed within pairs of points, involves explicitly collecting pairs of points restricted to individuals. Specifically, the pairs of points are chosen such that the *individual pairs of points always originate from the same individual*, and then these *sets* of pairs of points are conjoined such that the PDFs can be estimated. Thus, this method mixes individuals by including pairs of points from many individuals, but *does not mix individuals by pairing points from differing individuals.*

To concretely specify what intra-source aggregation means, begin with the time series:

$$(x_{11}, x_{12}, \cdots, x_{1n}, x_{21}, \cdots, x_{Nn}) \tag{5}$$

where, given an $x_{ij}$, $i$ specifies the individual, $j$ specifies the time, and a time-delay of $\tau$ for which the TDMI is to be calculated. The intra-source pairs that will be aggregated and used for estimating the PDF are then:

$$\begin{array}{c}
(x_{1,1}, x_{1,\tau}) \\
(x_{1,2}, x_{1,1+\tau}) \\
\vdots \\
(x_{1,n-\tau}, x_{1,n}) \\
(x_{2,1}, x_{2,\tau}) \\
\vdots \\
(x_{2,n-\tau}, x_{2,n}) \\
\vdots \\
(x_{N,n-\tau}, x_{N,n})
\end{array} \tag{6}$$

Thus, denote the *left* column by $X_1^{n-\tau}$ and the *right* column by $X_\tau^n$. Moreover, denote the TDMI calculated between these two columns as $I(X_1^{n-\tau}; X_\tau^n)$.

Much of the rest of this paper is dedicated to quantifying the implications and interpretations for when, and conditions under which the average and aggregate TDMIs differ. However, by comparing average to aggregate TDMI we will also see that, very often (but not always), the aggregate TDMI will form an upper bound on the TDMI of an individual.

## IV. TDMI-SPECIFIC ESTIMATOR BIASES

All statistical estimates have bias associated with them. Here we focus on three sources of bias that are particular to the estimation of the TDMI for a population: (i) sample-size-dependent estimator bias effects for the average versus the aggregate TDMI; (ii) the basic methodology we use for numerically estimating the bias for the TDMI calculation; and (iii) a source of non-estimator bias that is particular to the TDMI aggregation case — a sort of filtering bias.

### A. Sample size dependent estimator bias effects

A *practical* reason why the *order of aggregation* matters for estimating probability densities lies in the fact that most probability density estimation techniques have *estimator bias* that is, to first order, proportional to one over the number of points to a power of at least one. Thus, because we are interested in coping with populations of poorly measured individuals, and because we are comparing two methods of conjoining those individuals, it is important to understand how the number of data points will broadly affect estimator bias in the average and aggregate TDMI calculations.

Begin with a more computationally minded definition of the TDMI for a single time-series from a single source with $n$ points:

$$I[X_i(t); X_i(t-j)] = I_{X_i}(n) + B_E(n) \tag{7}$$

where $I_{X_i}(n)$ is the estimated TDMI for the $n$ pairs of points of $X$ and $B_E(n)$ is the total estimator bias of the calculation with $n$ pairs of points. Note that while explicit bias calculations for the entropy and TDMI calculations can be found in Refs. [21], [22], and [19], it will suffice to notice that for most PDF estimators (i.e., for kernel density estimators, or histogram style estimators), the bias estimates will follow:

$$B_E(n) \sim n^{-1} \tag{8}$$

Nevertheless, it is worth noting that there is also a estimator-specific, bandwidth-specific factor on $B_E(n)$ that is dependent on the *proportion of support* (e.g., number of bins) for which there exist no data points, and this factor can be important when $n$ is small (c.f., [22] where this effect is carefully quantified for the histogram estimator). To see how the bias of averaging TDMI over the population versus the bias of the TDMI for the pre-PDF-estimation aggregated populations differ, partition the time-series of length $n$ into $m$ pieces, where $\frac{n}{m}$ is a positive integer (thus, $m$ divides $n$ evenly and $n \geq m$). Now, consider the difference between $I[X_i(t), X_i(t-j)]$ calculated on *a single* time-series of length $n$ , and $I[X_i(t), X_i(t-j)]$ calculated on $m$ disjoint time-series of length $\frac{n}{m}$ and then averaged. More specifically, consider:

$$I = I[X_i(t), X_i(t-j)] = I_{X_i}(n) + B_E(n) \tag{9}$$

versus

$$I' = \frac{1}{m}\sum_{i=1}^{m} I_{X_i}(n/m) + B_E(n/m) \tag{10}$$

Now, if the bias, $B_E$, scaled linearly in the number of points, $n$, then the bias contribution of Eq. 9 will be the same as the bias contribution of Eq. 10. However, we know the bias obeys a power-law in the number of points, $n$, so we get the difference between bias estimates to at least be:

$$\delta B_E = (\frac{1}{m}\sum_{i=1}^{m} B_E(n/m)) - B_E(n) \tag{11}$$

$$\sim \frac{m-1}{n} \tag{12}$$

where $\delta B_E > 0$ for all $m > 1$. Or, said differently,

$$\frac{1}{m}\sum_{i=1}^{m} B_E(n/m) \geq B_E(n) \tag{13}$$

where equality is satisfied only when $m$ is one, or when the population consists of a single element. Note that when the population is particularly poorly sampled, say one or two measurements per element of the population, then $m \approx n$ and thus the *difference in the bias* of the population average versus the aggregated population will be will be order one. More importantly, *averaging the MI of many poorly sampled individuals* will not help the MI converge to its bias-free, high cardinality estimate.

Aside from the overall effect of $n$, there are other small sample size effects, and these effects can have profoundly different outcomes depending on the estimator. For instance, in the presence of few points, a KDE estimator will often, in the name of smoothing, over-estimate the probability for empty portions of the support, resulting in a PDF estimate that is closer to a uniform random variable. Thus, a KDE-PDF based TDMI calculation will likely *underestimate* the TDMI. In contrast, a histogram estimator will underestimate the probability for empty portions of the support, thus yielding a more sharply peaked distribution that will yield an over-estimate of the TDMI. Because of these opposing effects, it is possible to verify the existence of finite-size effects by simply observing the difference between the KDE and histogram estimated TDMI estimates for the same data set.

In the end, because we are working to understand how to estimate the TDMI in the context of large, poorly measured populations, there will be a significant advantage to aggregating populations *before* estimating the PDFs necessary to carry out the TDMI calculations from the perspective of estimator bias minimization.

### B. Fixed point bias estimate for average and aggregate populations

The fixed point TDMI bias estimation method [19] attempts to estimate the $\tau = \infty$ TDMI by randomly permuting the time-ordering of one of the sets of pairs used to estimate the distributions for a given $\delta t$ or $\tau$. Fundamentally, there are two different methods for estimating the TDMI fixed point (if it exists), random permutation *within the individuals* (i.e., not mixing individuals), and random permutation *over the entire population*, thus intermixing individuals.

The first method, *individual-wise random permutation* (IRP), involves randomly permuting the temporal ordering of one column (without replacement) of the data set used to estimate the distributions *without intermixing individuals*, or:

$$B_{IRP}(\tau, n) = \lim_{Z\to\infty} \frac{1}{Z}\sum_{i=1}^{Z} I(X_1^{n-\tau}, \mathcal{X}_\tau^n(i,t)) \tag{14}$$

where $\mathcal{X}_n^\tau(i,t)$ is the $i^{th}$ random permutation (without replacement) of the *left index* of the column vector $X_\tau^n$ (i.e., do not permute the first index of $x_{i,j}$ from equation 6). The IRP-method random permutation occurs *only within an individual* and not across the population, thus destroying information about only time-based correlations while preserving inter-individual information. Finally, there will exist a IRP bias estimate for both the average and aggregate TDMI cases, $\bar{B}_{IRP}$ where Eq. 14 is specified for a single individual and then averaged over the population, and $\hat{B}_{IRP}$ which is specified exactly as per Eq. 14.

The second method, *population-wide random permutation* (PRP), which exists only in the aggregated population context, involves randomly permuting, without regard to the individual, one column of the *entire populations'* data set used to estimate the PDFs or,

$$\hat{B}_{PRP}(\tau, n) = \lim_{Z\to\infty} \frac{1}{Z} \sum_{i=1}^{Z} I(X_1^{n-\tau}, \mathcal{X}_\tau^n(i, N, t)) \tag{15}$$

where $\mathcal{X}_n^\tau(i, N, t)$ is the $i^{th}$, random permutation (without replacement) of the *both indices* of column vector $X_\tau^n$. Because the PRP estimate intermixes both the population and time, the PRP destroys information about *both* intra-individual time correlations *and* inter-individual information (i.e., information about differences in normalization or the supports). In the context of a single source, $\bar{B}_{IRP} = \hat{B}_{IRP}(n) = \hat{B}_{PRP}(n)$. Similarly, when the population is both relatively uniform over both the PDFs and the support of the PDFs, then the PRP bias estimate will be equivalent to the bias estimate of the IRP, and thus can be thought of as an estimate of the estimator bias. However, if the support of the PDFs over the population is not uniform (i.e., if the support of any of the individuals of the population differs from the support of the population), then the PRP bias estimate will differ from the IRP bias estimate (we will discuss this explicitly in section VI A). Note that $\bar{B}_{IRP}$, $\hat{B}_{IRP}$, and $\hat{B}_{PRP}$ are dependent on both $\tau$ or $\delta t$ (because of the filtering effect discussed in the next section) and $n$, the number of points used in the estimate. In general, we will drop the $n$ from the notation, and when there is not a $\tau$ or $\delta t$ dependence, we will not include it in the notation (in general, for the data sets and $\delta t$'s we consider in this paper, there is not a strong $\delta t$ dependence).

### C. Non-estimator bias: how the TDMI calculation can act as a population filter

While it is clear that the TDMI calculation only applies to the data used to estimate the PDFs, it is less obvious that *the act of constructing the data sets used to estimate the PDFs* can *filter out substantial portions of the overall population.* Specifically, because construction of the data sets for the PDF estimation involves collecting all *pairs* of points separated by some time $\tau$ or $\delta t$, if some individuals do not have *pairs* of points separated by $\tau$ or $\delta t$, those individuals will be filtered out of, or excluded from, the data set used to estimate the PDFs and thus the TDMI. In this sense, the TDMI calculation *implicitly filters the population by measurement frequency*; this is not an externally imposed data constraint, it is simply a result of calculating the TDMI in the context of population whose elements do not have identical measuring frequencies.

To understand how this filtering bias can affect the results, consider a polarized example population made up of two differently measured subsets of individuals. Specifically, the first subset of the population has individuals sampled once an hour for a month and the second subset of the population has individuals sampled once a month for 20 years. These two population represent patients with acute and chronic conditions, respectively. If the TDMI of the population is calculated for any $\delta t$ less than a month, only data set one will be represented. Similarly, if the TDMI is calculated for $\delta t$ of a month or greater, only data set two will be represented. When plotting the TDMI graph versus $\delta t$, the graph has, in a sense, a bias. Namely, two the graph represents two disjoint populations for $\delta t >$ one month.

Of course, for real EHR data, even more complicated problems can appear when the same individual is sampled at different rates *depending on the statistical state of the individual* (e.g., a patient with a chronic and acute condition). This problem is particularly acute for health care data because health correlates with presence of measurement — healthy patients are not measured often while sick patients are — thus leading to the possibility of having different subpopulations or statistical states being filtered out when calculating the TDMI for some $\delta t$ values.

Thus, when estimating a TDMI for a population, it is important to quantify both who is populating the data set *explicitly used* to estimate the PDFs *and* how the proportionality of the subpopulations changes in the set used to estimate the PDFs as the delay is changed. If the population and proportionality of subpopulations in all the $\delta t$ or $\tau$ TDMI estimates does not change, then the bias estimates are *independent of the delay.*

#### 1. Methods for assessing $\delta t$ bin compositions

To quantify the composition of the data set, begin with the following notation: (i) $b_i(\tau)$ represents the number of pairs of points in the $\tau$ time bin contributed by individual $i$; (ii) $b_{max}(\tau) = N_{max}$ and $b_{min}(\tau) = N_{min}$ correspond to the maximum and minimum number of pairs of points, over all individuals, present in the data set; $N_*$ represents the sum of $b_i(\tau)$, or the total number of pairs of points in the data set; (iii) $N$ represents the total number of individuals in the population; and (iv), $\varsigma(\tau)$ represents the set of indices of individuals monotonically ordered by increasing $b_i$. Based on these quantities, define the following functions:

$$\Theta(\varsigma(\tau)) = b(\varsigma), \tag{16}$$

$$\tilde{\Theta}(\tilde{\varsigma}(\tau)) = \frac{b(\frac{\varsigma(\tau)}{M})}{b_{max}} \tag{17}$$

noting that $\tilde{\Theta}(\tau)$ [27] is $\Theta(\tau)$ normalized to lie on the unit square. Next, define the following integral that quantifies the population composition of the data set:

$$H_{\tilde{\Theta}}(\tau) = \int_{\tilde{\varsigma}} \tilde{\Theta} d\tilde{\varsigma}. \tag{18}$$

When the time series of the members of the population are both uniformly sampled and of the same length, $H_{\tilde{\Theta}}(\tau)$ will be equal to one; thus the closer $H_{\tilde{\Theta}}(\tau)$ is to one, the more composition of the data set includes the entire population uniformly, while the closer $H_{\tilde{\Theta}}(\tau)$ is to zero, the more composition of the data set represents a small subset of the population (possibly only an individual). A second, more gross quantification of how the population is represented in TDMI data set at a fixed $\delta t$ is the percentage of individuals that contribute at least one pair to the data set, or:

$$H_{b_i \neq 0}(\tau) = \frac{\#(b_i \neq 0)}{N} \tag{19}$$

Note that an alternative, highly related quantity we have found useful is the cumulative distribution function (CDF) of the $b_i$'s.

Finally, while it is tempting to think of the population makeup of the $\tau$ data set as a measure of homogeneity within a population, this interpretation is sometimes, but not always, correct. What $H_{\tilde{\Theta}}(\tau)$, $H_{b_i \neq 0}(\tau)$, or any other like-minded metric really detail is how a population is measured and thus represented in a given $\tau$ or $\delta t$ bin. Specifically, when *measurement frequency* is correlated with statistical state or dynamics, then it is likely that $\tau$ bins will filter a population and make it more homogeneous. However, it is easy to think of examples where *measurement frequency* is random, or uncoupled from a statistical state or dynamics, and in this case, all the diversity of the population will be present in any given $\tau$ time bin.

## V. POPULATION-BASED DEVIATIONS FROM THE INDIVIDUAL TDMI ESTIMATES

### A. Heterogeneity-based deviations from the individual: average TDMI case

To understand how representative the *average MI* over the population is of an individual in the population, begin by setting $p_1$ as the PDF that most resembles the *average* (choosing $p_1$ to be the median among the $p_i$'s would work as well) among the set of $p_i$'s *relative to the abstract support*, $\mathcal{S}$; note that the average PDF is defined by:

$$\bar{p} = \frac{1}{N} \sum_{i=1}^{N} p(X_i[\tau]). \tag{20}$$

Note that in this situation, every $p_i$ has the same abstract support (by definition), which we will denote as $\bar{\mathcal{S}}$. Further, note that it is possible to have a set of $p_i$'s such that no $p_i$ resembles the mean *graph* of the $p_i$'s. Next, relative to $p_1$ we can now relate each $p_i$ to $p_1$ as follows:

$$p_i = p_1(\bar{\mathcal{S}}) - \bar{\epsilon}_i(\bar{\mathcal{S}}) \tag{21}$$

where $\bar{\epsilon}_i(\bar{\mathcal{S}})$ is distance between the *graphs* of $p_1$ and $p_i$ at a given value in $\bar{\mathcal{S}}$. Recalling the definition of the TDMI, we get:

$$\begin{aligned} & I[X(t); X(t+\tau)] = \\ & \bar{I}(\tau) = \frac{1}{N} \sum_{i=1}^{N} \int p(X_i(j), X_i(j-\tau)) \\ & \log(\frac{p(X_i(j), X_i(j-\tau))}{p(X_i(j))p(X_i(j-\tau))}) dX_i(t) dX_i(t+\tau) \\ & = \int \bar{\iota}(\tau) dX(t) dX(t+\tau). \end{aligned} \tag{22}$$

Now, because integration is a linear operation, focus on the integrand instead, or more specifically, focus on:

$$\begin{aligned} & \bar{\iota}(\tau) = \\ & \frac{1}{N} \sum_{i=1}^{N} p(X_i(j), X_i(j-\tau)) \log(\frac{p(X_i(j), X_i(j-\tau))}{p(X_i(j))p(X_i(j-\tau))}) \\ & = p(X_1(j), X_1(j-\tau)) \log(\frac{p(X_1(j), X_1(j-\tau))}{p(X_1(j))p(X_1(j-\tau))}) \\ & + \bar{G}(N, \epsilon_i, p(X_1(j), X_1(j-\tau)), p(X_1(j)), p(X_1(j-\tau))) \\ & = \bar{\rho}(\tau) + \bar{G}(\tau) \end{aligned} \tag{23}$$

where, $\bar{G}(\tau)$ is given by:

$$\begin{aligned} & \bar{G}(\tau) = \\ & \quad - \frac{1}{N} [\sum_{i=1}^{N-1} \left( \frac{\bar{\epsilon}_i}{p(X_1(j), X_1(j-\tau))} \right) \\ & \quad \left( \log \frac{p(X_1(j), X_1(j-\tau))}{p(X_1(j))p(X_1(j-\tau))} \right) \\ & \quad + \log \left( \frac{1 - \frac{\bar{\epsilon}_i}{p(X_1(j), X_1(j-\tau))}}{(1 - \frac{\bar{\epsilon}_i}{p(X_1(j))})(1 - \frac{\bar{\epsilon}_i}{p(X_1(j-\tau))})} \right) \\ & \quad \left( \frac{\bar{\epsilon}_i}{p(X_1(j), X_1(j-\tau))} - 1 \right) ] \end{aligned} \tag{24}$$

(for a more explicit calculation of $\bar{I}$, c.f., appendix A 1). As each $\bar{\epsilon}_i$ goes to zero, $\bar{G}$ goes to zero; thus the more *support independent* variance (recall $\bar{\epsilon}_i$ is relative to the abstract support $\bar{\mathcal{S}}$) there is within the population, the larger $\bar{G}$ will be, and the less $\bar{I}(\tau)$ will represent the TDMI of an individual element within the population. Written explicitly, $\bar{I}(\tau)$ represents the "average" individual *plus* the *sum of the deviations from that individual.*

#### 1. *Entropy of the averaged population*

While the primary topic in this paper is the TDMI, we will contend briefly with the TDMI for $\tau = 0$, or the auto information. Based on an identical means of calculation, the information entropy of a time series for a population can be defined as follows:

$$\bar{h}_I = -\frac{1}{N}\int [p_1 \log(p_1) + p_1 \sum_{i=1}^{N-1} \log(p_1 - \bar{\epsilon}_i) - \sum_{i=1}^{N-1} \epsilon_i \log(p_1 - \bar{\epsilon}_i)]dx \tag{25}$$

Thus, when $\bar{\epsilon}_i \to 0$, the $h_I$ for the population *relative to the abstract support* tends toward the information contained in an individual.

### B. Heterogeneity-based deviations from the individual: aggregate TDMI case

To understand how the diversity in the population is rendered via the TDMI of the *aggregated population* begin by recalling that the TDMI for the aggregated set is defined by:

$$\begin{aligned} \hat{I}(\tau) =& I(X_1^{n-\tau}; X_\tau^n) \\ =& \int p(X_1^{n-\tau}; X_\tau^n) \log(\frac{p(X_1^{n-\tau}; X_\tau^n)}{p(X_1^{n-\tau})p(X_\tau^n)}) dX_1^{n-\tau} dX_\tau^n \\ =& \int \hat{\imath}(\tau) dX_1^{n-\tau} dX_\tau^n \end{aligned} \tag{26}$$

where, under ideal (single, stationary source) circumstances the PDF of the aggregated density obeys

$$\hat{p}(X_1^{n-\tau}; X_\tau^n) = \frac{1}{N}\sum_{i=1}^{N} p(X_1^{n-\tau}(i); X_\tau^n(i)) \tag{27}$$

where $X_1^{n-\tau}(i)$ and $X_\tau^n(i)$ represent the PDF restricted to individual $i$. Intuitively, Eq. 27 just says that we are creating the aggregate PDF by summing the *graphs* of all the individuals *relative to the union of the supports of all the individuals*, that is, relative to $\hat{S} = \cup_{i=1}^N \hat{S}_i$.

To choose a PDF that most closely resembles a centroid, it is helpful to have a concept of abstract support; however, because $\hat{I}(\tau)$ is defined relative to the actual support of the *population*, the individual population PDFs do not separate as naturally as in the $\bar{I}(\tau)$ case. Nevertheless, conceptually, to define an abstract support in the aggregate circumstance, one needs to, in spirit, construct a situation where all the PDFs have roughly the same range or support. There are several ways one can imagine achieving such goal; here will define the *abstract support*, $\hat{\mathcal{S}}$, such that every patient has been renormalized to have the identical support — the unit interval (i.e., $[0, 1]$). It is important to realize that relative to the aggregate case there can be a very severe difference between the TDMI of an aggregated population defined on support of the $\hat{S}$ versus the abstract support $\hat{\mathcal{S}}$. To allow for quantifying these potential differences, define the TDMI for an aggregated population relative to the abstract support, $\hat{\mathcal{I}}(\tau)$. Now, using the abstract support, select $p_1$ in the same way we selected $p_1$ in the previous section, by selecting the PDF that most closely represents the mean over the population of PDFs *relative to the abstract support.* This definition implies an important difference in how $p_i$ is specified in the aggregate case versus the average case because, despite the fact that we use an abstract support to select a $p_1$, $\hat{I}(\tau)$ is *not* calculated relative to the abstract support, and thus the differences between $p_1$ and $p_i$ are instead defined by:

$$p_i = p_1(\hat{S}) - \hat{\epsilon}_i(\hat{S}) \tag{28}$$

where $\hat{\epsilon}_i(\hat{S})$ is distance between the *graphs* of $p_1$ and $p_i$ at a given value in *total support*, $\hat{S}$. Next, focusing on the integrand, $\hat{\imath}$, and substituting Eq. 28 into Eq. 27 and recalculating $\hat{\imath}$ we arrive at (dropping the subscript on $p_1$):

$$\begin{aligned} \hat{\imath}(\tau) =& p(X_1^{n-\tau}; X_\tau^n) \log(\frac{p(X_1^{n-\tau}; X_\tau^n)}{p(X_1^{n-\tau})p(X_\tau^n)}) \\ &+ \hat{G}(\tau)(N, \hat{\epsilon}_i, p(X_1(j), X_1(j-\tau)), p(X_1(j)), p(X_1(j-\tau))) \\ &= \hat{\rho}(\tau) + \hat{G}(\tau) \end{aligned} \tag{29}$$

where $\hat{G}(\tau)$ is explicitly given by:

$$\begin{aligned} \hat{G}(\tau) =& \log\left(\frac{1 - \frac{\sum_{i=1}^{N-1}\hat{\epsilon}_i}{Np(X_1^{n-\tau}, X_\tau^n)}}{(1 - \frac{\sum_{i=1}^{N-1}\hat{\epsilon}_i}{Np(X_1^{n-\tau})})(1 - \frac{\sum_{i=1}^{N-1}\hat{\epsilon}_i}{Np(X_\tau^n)})}\right) \\ & \left(p(X_1^{n-\tau}, X_\tau^n) - \frac{\sum_{i=1}^{N-1}\hat{\epsilon}_i}{N}\right) \\ & - \frac{\sum_{i-1}^{N-1}\hat{\epsilon}_i}{N} \log\left(\frac{p(X_1^{n-\tau}, X_\tau^n)}{p(X_1^{n-\tau})p(X_\tau^n)}\right) \end{aligned} \tag{30}$$

(for a more explicit calculation of $\hat{G}$ and $\hat{I}$, c.f., appendix A 2). Thus, as the *average of the* $\hat{\epsilon}_i$'s go to zero, $\hat{G}(\tau)$ will go to zero; moreover, when *both* the width of the band of PDFs decreases and when the supports of the distributions overlap (i.e., when $\cap_{i=1}^N \hat{S}_i \to \cup_{i=1}^N \hat{S}_i$), the TDMI of the aggregate population ($\hat{I}$) will represent an individual within a homogeneous population (because the individuals within the population are similar). Similarly, when either the width of the band of PDFs increases or the supports of the distributions becomes disjoint, (i.e., when $\cap_{i=1}^N \hat{S}_i \to 0$), $\hat{I}(\tau)$ will represent the TDMI within the diverse population. Or, said differently, the TDMI for the aggregated population will represent the TDMI of the *population* plus the *sum of the individual based differences from the population.* As we will see in the sections that follow, this second circumstance can lead to subtle difficulties in interpretation. Finally, note that the calculation that yielded $\hat{\imath}$ does not explicitly depend on the support; the explicit $\hat{\epsilon}$'s will differ between $\hat{I}(\tau)$ and $\hat{\mathcal{I}}(\tau)$, but the explicit form of $\hat{\imath}$ will not.

#### 1. Entropy of the aggregated population

Again, while the TDMI is the primary topic of this paper, in both the interest of completeness and later analysis, we define $h_I$ for the aggregated population, which was calculated in analog with $\hat{I}$, as follows:

$$\begin{aligned}\hat{h}_I = &- \int p \log(p - \frac{\sum_{i=1}^{N-1} \hat{\epsilon}_i}{N}) \\ &- \frac{\sum_{i=1}^{N-1} \hat{\epsilon}_i}{N} \log(p - \frac{\sum_{i=1}^{N-1} \hat{\epsilon}_i}{N})\end{aligned} \tag{31}$$

In contrast to the situation where the information entropy is averaged over the population, when the average $\frac{\hat{\epsilon}_i}{N} \to 0$, the information entropy for the aggregated population, $\hat{h}_I$, *relative to the real support of the population* tends toward the information contained in an individual who has the most data pairs in the PDF estimate.

## VI. HOW TO INTERPRET THE TDMI FOR A POPULATION, OR, TDMI-BASED METHODS FOR INTERPRETING POPULATION DIVERSITY

To achieve a practical understanding of the meaning of the TDMI in the context of a population, we have to combine information from the previous section to construct an explicitly numerically computable means of interpreting $\bar{I}(\tau)$ and $\hat{I}(\tau)$. Practically speaking, there are two broad situations: (i) $\bar{I}(\tau)$ is practically calculable (when $\bar{I}(\tau)$ is calculable, $\hat{I}(\tau)$ always will be); and (ii), $\bar{I}(\tau)$ is not calculable (usually to estimate $\bar{I}(\tau)$ there need to be at least 100 *pairs of points* per representative element) leaving us only with $\hat{I}$-related quantities. Relative to the first situation, define the difference between $\bar{I}(\tau)$ and $\hat{I}(\tau)$, or

$$\begin{aligned}\delta I(\tau) &= |\bar{I}(\tau) - \hat{I}(\tau)| \\ &= |\int_{\bar{S}} p_1(\bar{\mathcal{S}}) - \int_{\hat{S}} p_1(\hat{S})| + |\int_{\bar{\mathcal{S}}} \bar{G} - \int_{\hat{S}} \hat{G}| + (\bar{B} - \hat{B})| \\ &= \delta\rho + \delta G_{\int} + \delta B\end{aligned} \tag{32}$$

This allow for the following conjecture which we will not proven in this paper:

**Conjecture 1** *In the circumstance where $\bar{I}(\tau)$ can be accurately estimated, $\delta I(\tau) \sim 0$ if and only if the population used to estimate $\bar{I}(\tau)$ and $\hat{I}(\tau)$ is statistically homogeneous temporally (i.e., the PDFs representing the individuals in the population are identical, as are the PDFs under temporal evolution).*

The forward direction of the if and only if statement, that $\delta I(\tau) \neq 0$ implies a heterogeneous population will be briefly discussed in section VI B; this direction is more complicated to prove. The reverse direction of the if statement in this conjecture claims that if the population represents a single, stationary, homogeneous distribution then $\delta I(\tau) \sim 0$; this claim relies on the fact that in this circumstance all $\epsilon$'s are zero and thus $\bar{I}(\tau)$ (Eqn. 22) and $\hat{I}(\tau)$ (Eqn. 26) represent a homogeneous source and are equivalent up to bias. Essentially, when one can estimate $\delta I(\tau)$, one can interpret the population make-up *without* delving deeply into the detailed *sources* of the TDMI. In contrast, when only $\hat{I}(\tau)$ is practically calculable, the interpretation of $\hat{I}(\tau)$ can only be understood though understanding the *source* of the TDMI. Nevertheless, in general, it is insightful to understand the sources of the TDMI, and the sources of the TDMI are tied to the make-up of the population.

From a detailed perspective, the make-up of the population is important because the deviation of the TDMI from the homogeneous case is due to non-zero $\epsilon$'s, and the source of non-zero $\bar{\epsilon}$'s can differ from the source of non-zero $\hat{\epsilon}$'s. Specifically, $\bar{\epsilon}$ can *only* be non-zero because of differences between the graphs of the $p_i$'s. This is because *all the $p_i$s for the average TDMI have the same support.* In contrast, the source of non-zero $\hat{\epsilon}$'s is due to a heterogeneous population can be split into three broad categories: (i) differences in the TDMI estimates due to differences in the supports *independent* of the graphs of the PDFs; (ii) differences in the TDMI estimates due to differences in the graphs *independent* of the supports; and (iii), differences in the TDMI estimates due to the supports' *effect on the graphs.*

### A. Support dependent, graph independent, effects on the population TDMI

To understand and *quantify* the differences in the TDMI estimates due to differences in the supports *independent* of the graphs of the PDFs, consider the difference between the random permutation bias estimates defined in section IV B.

First, recall that the population-wide random permutation bias estimate will be roughly equivalent to the estimator bias, or $B_{PRP}(\tau) \approx B_E(\tau)$ regardless of the supports or densities of the elements (c.f., [19] for small sample size qualifications of this statement). Next, note that the individual-wise random permutation bias estimate, $\hat{B}_{IRP}(\tau)$ represents the *bias due to heterogeneity in the supports* plus the estimator bias. Thus, the contribution to the bias due to the diversity in population normalization is approximated by the difference between the individual-wise and population-wise random permutation bias estimates:

$$B_{RP}(\tau) = |\hat{B}_{PRP}(\tau) - \hat{B}_{IRP}(\tau)|. \tag{33}$$

There are two reasons why $B_{RP}(\tau)$ can be non-zero. First the number of points used to calculate the two can differ by orders of magnitude (say, a population of $1,000$ with 10 points each); in this case, $B_{RP}(\tau)$ represents the $1/n$ effect on the bias estimates. In the case

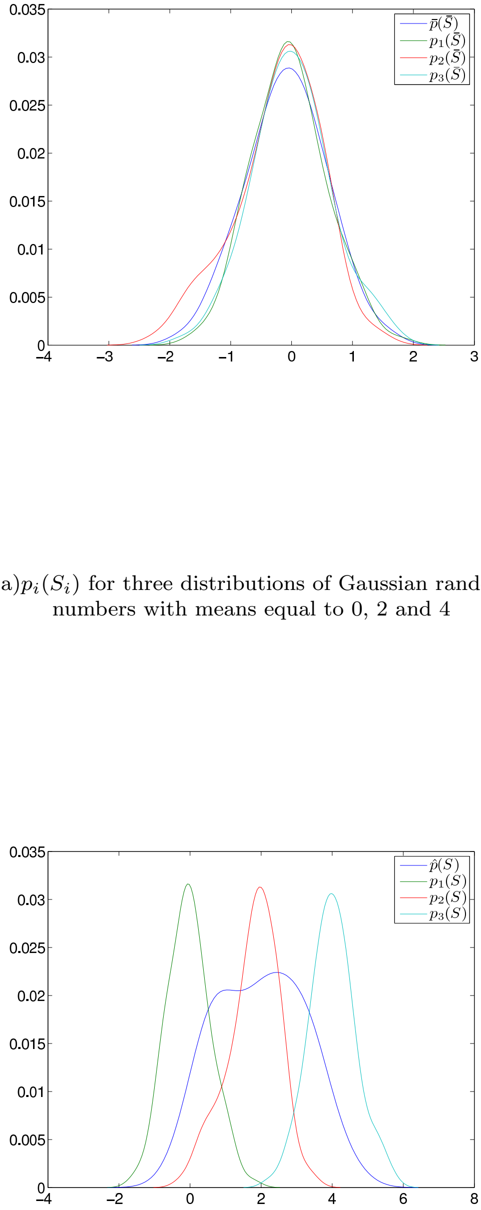

(a)$p_i(S_i)$ for three distributions of Gaussian random numbers with means equal to 0, 2 and 4

(b)$p_i(S)$ for three distributions of Gaussian random numbers with means equal to 0, 2 and 4 as well as $p(s) = 1/3 \sum_{i=1}^{3} p_i(\hat{S})$.

FIG. 1: Graphically comparing $\bar{p}$ (average PDF) and $\hat{p}$ (PDF of the aggregate) for a collection of three collections of Gaussian random numbers whose distributions have means 0, 2 and 4 respectively.

where the number of pairs used to estimate $\hat{B}_{PRP}(\tau)$ and $\hat{B}_{IRP}(\tau)$ are relatively similar (e.g., more than 100 and within an order of magnitude; to control for the number of points, it is easy reduce the cardinality of the set used to calculate $\hat{B}_{PRP}(\tau)$) Fig. 1(b) shows visually how these bias estimates would render differently. In this context, $\hat{B}_{IRP}(\tau)$ would be identical to $I$, where as randomly permuting the entire population, such as is done to estimate $\hat{B}_{PRP}(\tau)$, will result in one of the marginal distributions becoming $\hat{p}(\hat{S})$ — a uniform distribution instead of three Gaussians with distinct means — thus greatly changing the amount of mutual information. These effects are primarily support-driven effects; note that while it is possible that differences in the underlying distribution function can be rendered through $B_{RP}(\tau)$, differences in the support of those distributions will always be rendered through $B_{RP}(\tau)$. As we will see in a moment, $B_{RP}(\tau) \approx \hat{B}_{IRP}(\tau)$ is *not enough* to imply that $\delta I(\tau) \approx 0$, but is enough to imply that the variance in the boundaries of the supports will all be relatively small. Nevertheless, while in some circumstances it may be difficult to use the bias estimates to detect a difference in the average versus aggregate TDMI, we can use the bias estimates to interpret the average and aggregate TDMI signal. In particular, when $B_{RP}(\tau) \leq B_E(\tau)$, intermixing individuals' measurements has no effect on the random permutation bias estimate, implying that there is very little population selection information in the TDMI estimate. Thus, $B_{RP}(\tau) \leq B_E(\tau)$ *at least* implies overlapping distribution supports. Similarly, when $B_{RP}(\tau) \gg B_E(\tau)$, intermixing elements has a profound effect on the random permutation bias estimates; in this instance, $B_{RP}(\tau)$ reveals a bias whose source is the diversity of the supports among the elements. This leads us to the measure of homogeneity of supports that is very computable even for poorly measured populations (e.g., when only $\hat{I}(\tau)$ is calculable); the *TDMI homogeneity of support* is defined by the following equation:

$$\mathcal{H}_S(\tau) = \frac{|\hat{B}_{IRP}(\tau) - \hat{I}(\tau)|}{\hat{I}(\tau)} \tag{34}$$

The closer $\mathcal{H}_S(\tau)$ is to one, the less the diversity of the supports over the population; similarly, the closer $\mathcal{H}_S(\tau)$ is to zero, the greater the diversity of the supports over the population. (Again, note one must control for the dependence on the number of pairs used to estimate the above quantities.)

It is worth noting that a similar analysis can by done by comparing $\hat{\mathcal{I}}(\tau)$ to $\hat{I}(\tau)$, as their difference will reveal support based effects. The principles behind a $\delta\hat{I}(\tau) = |\hat{\mathcal{I}}(\tau) - \hat{I}(\tau)|$ and $\mathcal{H}_S(\tau)$ are similar in that they both address normalization of support based effects, only $\mathcal{H}_S(\tau)$ depends on quantities that represent distributions — $\hat{B}_{IRP}(\tau)$ and $\hat{B}_{PRP}(\tau)$ can both be estimated many times — and thus are likely more robust.

### B. Graph dependent, support independent, effects on the population TDMI

To understand in detail how differences in the graphs *independent* of the supports can affect the $\bar{I}(\tau)$ and $\hat{I}(\tau)$, begin by assuming that all the $p_i$'s *have the same support*, or that $\cap_{i=1}^{N} S_i = \cup_{i=1}^{N} S_i$. In this circumstance, the $\bar{\epsilon}_i = \hat{\epsilon}_i$ for all $i$. Thus, the contribution of the diversity of PDFs within the population to $I$, or the deviation from the mean at a particular $x \in S$ value, is captured by $\bar{G}(\tau)$ and $\hat{G}(\tau)$ as defined in Eqs. 24 and 30. Consequently, the only way that $\bar{I}(\tau)$ can be different from $\hat{I}(\tau)$ up to the estimator bias is for the variation in the collections of PDFs to be due to the *order of averaging* as rendered though the $G$'s.

Based on the aforementioned intuition, we claim (e.g., conjecture 1) that $\delta I(\tau)$ is equal to zero if and only if all the $\epsilon$'s are zero. While we will not present a qualified proof of this claim here, we can offer an intuitive argument as to why our claim is justified. First note that by inspection, if $\epsilon_i = 0$ for all $i$, $\delta G(\tau) = \bar{G}(\tau) = \hat{G}(\tau) = 0$. Now, what remains is to understand what happens to the $G$'s when there are non-zero $\epsilon$'s; to do this, note that we reduce the $G$'s to the terms they do not have in common:

$$\bar{G}(\tau) \sim \bar{g}(\tau) = (p_{i\tau} - [\epsilon]) \log(\frac{1 - \frac{[\epsilon]}{p_{i\tau}}}{(1 - \frac{[\epsilon]}{p_i})(1 - \frac{[\epsilon]}{p_\tau})}) \qquad (35)$$

$$\hat{G}(\tau) \sim \hat{g}(\tau) = \frac{1}{N p_{i\tau}} \sum_{j=1}^{N} (p_{i\tau} - \epsilon_j) \log(\frac{1 - \frac{\epsilon_j}{p_{i\tau}}}{(1 - \frac{\epsilon_j}{p_i})(1 - \frac{\epsilon_j}{p_\tau})}) \qquad (36)$$

and then consider the difference in these quantities:

$$\delta G \sim \delta g(\tau) = |\bar{g}(\tau) - \hat{g}(\tau)|. \qquad (37)$$

Now, further noting that $\bar{g}(\tau)$ is convex (or concave, depending on the $p$'s) and applying standard convexity arguments, $\delta g$ will not equal zero unless $\epsilon_i = 0$ for all $i$. Thus, while it is possible that, through the act of integrating the $G$'s, symmetries will allow for the $G$'s to be equal, it is extremely unlikely. Moreover, because the convexity or concavity of $\bar{g}(\tau)$ depends on the nature of the $p$'s, it is difficult to say whether $\bar{g}(\tau)$ will be, in general, greater or less than $\hat{g}(\tau)$. Nevertheless, it appears in computational experiments that $\hat{g}(\tau)$ is often less than $\bar{g}(\tau)$. In any event, it is now more clear how diversity amongst the distribution of $p$'s over the same support can (and likely will) force $\delta I(\tau) \neq 0$.

In the situation where $\bar{I}(\tau)$ is not accessible, it may not be possible to fully understand the meaning of $\hat{I}(\tau)$. While $\mathcal{H}_S(\tau)$ can help identify support based effects, pure graph-based *temporally dependent* effects may be difficult to estimate. In particular, if the sample size for some of the individuals is small, then it will be difficult to determine the contribution to $\hat{I}(\tau)$ due to purely graphic diversity simply because there will be such high variance in the graphical PDF estimates due to small sample sizes[28]. In this case, the best that can be done is to estimate more static measures of graphic diversity such as those presented in section VII.

### C. Support dependent, graph-based effects on the population TDMI

There are two potential contributors to support dependent, graph-based effects on $\delta I(\tau)$, $\delta G(\tau)$ and $\delta\rho(\tau)$.

The contribution to $\delta I(\tau)$ due to $\delta\rho(\tau)$ is entirely due to the limits of integration; the integrand for the average and aggregate $\rho$ component of the TDMI are identical. Thus, intuitively, $\delta\rho > 0$ because of the *relative location* of the support of $p_1$ in reference to the total support of the population; $p_1$ will represent a *more peaked* distribution when defined on $\hat{S}$ compared to $\bar{S}$. Note that while $\delta\rho$ is, in general, computable, it has similar characteristics to $\mathcal{H}_S(\tau)$ with more severe bias issues.

The contribution due to $\delta G_{\int}$ is not as intuitive; to understand how diversity in the supports contributes to $\delta G_{\int}$ via the induced differences in the $\epsilon$'s, consider Figs. 1(a) and 1(b). Relative to Fig. 1(a), begin by defining $\bar{p}(\bar{\mathcal{S}})$ as the average of the PDFs relative to the abstract support, or $\bar{p}(\bar{\mathcal{S}}) = \frac{1}{3}(p_1(\bar{\mathcal{S}}) + p_2(\bar{\mathcal{S}}) + p_3(\bar{\mathcal{S}}))$; here all the $\bar{\epsilon}_i$'s will be small and independent of the support. This is how variation in the population is rendered when calculating $\bar{I}$, and thus how $\bar{G}$ will render. In contrast, define the average of the PDFs relative to the *total support*, or $\hat{p}(\hat{S}) = \frac{1}{3}(p_1(\hat{S}) + p_2(\hat{S}) + p_3(\hat{S}))$; this is the aggregate scenario. Here it is clear that *both* the averaged PDF will not resemble *any* of the PDFs *and* relative to a selected $p_1$. Moreover, all $\hat{\epsilon}_i$'s will be relatively large and on the order of the various $p_i(\hat{S})$'s over a non-trivial portion of the population support $\cup_{i=1}^{N} S_i$. Because of this, when the supports of the individuals differ, the largest term in $\hat{I}(\tau)$, $\hat{G}(\tau)$, will be accounting primarily for *variation within the distribution of the supports of the population*, rather than support-independent variation within the population. Moreover, when the supports of the individuals are relatively invariant, $\hat{I}$ will be independent of time even when the $I$ of an individual varies with $\tau$. In any event, the point is, variation in the supports of otherwise identical distributions affects how the distributions are rendered though the TDMI calculation.

Finally, when only $\hat{I}(\tau)$ is available, which implies the presence of individuals with too few pairs of points to accurately estimate a PDF and thus the TDMI, and when there are support-dependent graph-based effects in the TDMI, it will likely be difficult to separate the support dependent, graph-based effects from the support *independent* graph-based effects on the TDMI (e.g., on the structure of the temporal correlation).

## VII. NON-TDMI-BASED METHODS FOR INTERPRETING POPULATION DIVERSITY

In this paper, we claim that the TDMI-based analysis can be used to both detail nonlinear correlation in time *and* interpret the composition of the population to which that correlation pertains to (i.e., whether the TDMI reflects and individual/homogeneous population or a diverse population). To verify this claim, we require a set of methods for establishing a *baseline* that are independent of information-theoretic machinery and can be used to interpret the make-up of the population. We propose three different quantifications of homogeneity of a population: (i) homogeneity in measurement representation, which addresses the variance in the distribution of the number of measurements per element of the population; (ii) homogeneity in support, which addresses variation in the supports of each elements' distribution; and (iii) homogeneity in density, which addresses variation in the PDFs (or the graphs of the PDFs) over the population. *Note* that all but one of the methods for quantifying homogeneity are *independent of time*, and all are *independent of any time-based correlation structure* existent within the data set. Moreover, the homogeneity qualification methods we propose here are neither exhaustive nor particularly innovative; rather they are simple intuitive methods devised to interpret and confirm the TDMI-based results. Nevertheless, many of these methods are useful in their own right; moreover, at least one of the quantities we define here is required to supplement the TDMI analysis when very few measurements exist per individual. Finally, table I contains a summary of the ten TDMI-independent quantities are we use to verify the TDMI methodology.

### A. Homogeneity in measurement composition

To quantify *homogeneity in measurement composition*, begin with the following two quantities. First, consider the difference between the mean of the raw measurements over the population versus the mean of the individual-wise measurement means, or:

$$
\begin{aligned}
H_{\bar{x}} = & \left( \frac{1}{\sum_{k=1}^{N} n_k} \sum_{i=1}^{\sum_{k=1}^{N} n_k} x_i \right) \\
& - \left( \frac{1}{N} \sum_{k=1}^{N} \frac{1}{n_k} \sum_{i=1}^{n_k} x_{i+\sum_{j=0}^{k-1} n_j} \right)
\end{aligned}
\tag{38}
$$

where $n_k$ is the number of points contributed by individual $k$, $N$ is the number of individuals in the population, and $n_0 = 0$. Now, $H_{\bar{x}} \approx 0$ under two circumstances: (i) the distribution of $n_k$'s has zero or small variance, *regardless* of the collection of individual distributions; or (ii) each individual comes from an identical distribution. Second, consider the variance of the probability density

| non-TDMI-based quantities for characterizing a population | | |
|---|---|---|
| $H_{\bar{x}}$ | difference between the population and individual element means | $\sim$ 0 implies *either* (i) most elements have a similar number of measurements, or (ii) the individuals come from distributions with similar means; $\gg 0$ implies the converse |
| $V(f(n))$ | variance of the PDF of the number of measurements per individual | (i) $V \sim 0$, $H_{\bar{x}} \sim 0$ imply elements were measured similarly; $\gg 0$, $H_{\bar{x}} \sim 0$ implies elements measured at different rates; $\gg 0$, $H_{\bar{x}} \gg 0$ implies elements measured at different rates with differing source distributions. |
| $\bar{s}_{min}$ | $E[s_{min}(i)]$ | lower support boundary mean. |
| $\bar{s}_{max}$ | $E[s_{max}(i)]$ | upper support boundary mean. |
| $V_{s_{min}}$ | $Var(s_{min})$ | lower support boundary variance. |
| $V_{s_{max}}$ | $Var(s_{max})$ | upper support boundary variance. |
| $\lvert\bar{S}\rvert$ | $\bar{s}_{max} - \bar{s}_{min}$ | length of support mean. |
| $V_{\lvert\bar{S}\rvert}$ | $Var(\bar{s}_{max} - \bar{s}_{min})$ | length of support variance. |
| $H_{RA}$ | area between the (point-wise) least and greatest PDF graph | quantifies variance between the PDFs of the population; $\sim$ 0 implies element PDFs are homogeneous; very sensitive. |
| $V_S(p)$ | $\int_S E[(p(x))^2] - E[p(x)]^2 dx$, variance of the PDFs *relative to a specified support*, $S$ | $\sim$ 0 implies homogeneity in PDFs; larger $Var_S(f)$ implies greater heterogeneity in the PDFs. |
| $V_{\hat{S}}(p)$ | $V_S(p)$ calculated relative to the support of the aggregate population; $\hat{S} = \cup_{i=1}^{N} \hat{S}_i$; note that there does exist an aggregate normalized support, $\hat{\mathcal{S}}$, but we will not use this quantity here. | $V_{\hat{S}}(p)$ has the same interpretation as $V_S(p)$ in general, but has the potiental to *include* support-based effects. |
| $V_{\bar{\mathcal{S}}}(p)$ | $V_S(p)$ calculated relative to the abstract support of the population, $\bar{\mathcal{S}}$ | $V_{\bar{\mathcal{S}}}(p)$ has the same interpretation as $V_S(p)$ in general, but excludes support-based effects. |

TABLE I: Summary of all the non-TDMI based metrics used to assess homogeneity in a population (both among the graphs and the supports) used to verify the TDMI-type analysis.

of the number of measurements per individual:

$$V_{f(n)} = \mathrm{Var}(f(n)) \tag{39}$$

where $f(n)$ denotes the density of measurements per individual. Combining these two quantities we arrive at three cases: (i) $V_{f(n)} \sim 0$ implies that $H_{\bar{x}} \sim 0$, together implying that the elements were measured similarly — no insight into the original distributions can be made; (ii) $V_{f(n)} \gg 0$ and $H_{\bar{x}} \sim 0$ together imply that the elements were measured at different rates regardless of their source distributions (which can be identical); and (iii) $V_{f(n)} \gg 0$ and $H_{\bar{x}} \gg 0$ together implies that the elements were measured at different rates and likely have differing source distributions. Note, that in general, both of these metrics are rather sensitive to diversity in a population.

### B. Homogeneity in measurement distribution supports

To characterize *homogeneity in distribution support* we rely on a brute force homogeneity characterization technique. Begin by recalling that the support for element $i$'s distribution as $S_i = [s_{min}(i), s_{max}(i)]$. Given these sets, which are defined by the individuals' measurements, define the mean and variance of the support minima, maxima, and length by:

$$\bar{s}_{min} = E[s_{min}(i)] \tag{40}$$
$$\bar{s}_{max} = E[s_{max}(i)] \tag{41}$$
$$V_{s_{min}} = Var(s_{min}) \tag{42}$$
$$V_{s_{max}} = Var(s_{max}) \tag{43}$$
$$|\bar{S}| = \bar{s}_{max} - \bar{s}_{min} \tag{44}$$
$$V_{|\bar{S}|} = Var(\bar{s}_{max} - \bar{s}_{min}) \tag{45}$$

These quantities afford relatively simple representations. For instance, when the minima, maxima, and lengths for the population have small variance, the intersection of the supports will not differ significantly from the union of the support — meaning the supports overlap. While a large variance in any either the minima, maxima, or lengths implies that the supports differ significantly over the population.

### C. Homogeneity in the distribution of the graphs of the measurement PDFs

To specify *homogeneity in the PDF* of the population we will use two methods. Intuitively, all of the methods characterize, in one way or another, the *width* of the maximum and minimum band of PDFs of the population over the support of the entire population. Begin by defining the PDF for an individual by $p_i(x)$, the supremum of the PDFs of the population by $\max_i(p(x)) = p_M(x)$, and the infimum of PDFs of the population by $\min_i(p(x)) = p_m(x)$, over the union of the supports, $S = \cup_i^N S_i$. First, using the $L_1$ (pseudo) distance [29] we can define the *relative area* of the width of the band of PDFs by:

$$H_{RA} = \frac{\int_S |p_M(x) - p_m(x)| dx}{\int_S p_M(x) dx} \tag{46}$$

The relative area, $H_{RA}$ is literally the proportion of the supremum of the collection of PDFs that coincides with the infimum of the collection of PDFs. When $H_{RA}$ is close to one, the maximum distance between PDFs over the population occupies all the volume of the population-wide PDF. In other words, the population has at least two substantially different PDFs. Similarly, when $H_{RA}$ is near zero, this implies that the proportion of the area between the supremum and infimum over the collection of $p_i$'s relative to the total area occupied by the supremum of the $p_i$'s over the population is very small. Thus the *implication* of $H_{RA}$ being near zero is that the $p_i$'s are all nearly identical. *However*, this method is very sensitive to heterogeneity; *a single* individual's PDF differing from the rest of the population can maximize $H_{RA}$ at one. In contrast, the second method for evaluating the diversity in PDFs over the population quantifies diversity from a mean within the population by estimating the *variance of the PDFs at a given at a given* $x$ integrated over a given support ($S$), or

$$V_S(p) = \int_S E[(p(x))^2] - E[p(x)]^2 dx \tag{47}$$

*Note*, $V_S(p)$ can be estimated relative to *two different* supports, the union of the supports, or the abstract support. This is an $L_2$ flavored representation of the variation in PDFs; the variance of the $p_i$'s at a given $x$ is maximized when $p_i$'s are maximally orthogonal (in the sense of an inner product between the $p_i$'s) to one another, and minimized when the $p_i$'s are minimally orthogonal (meaning they coincide). Thus, $V_S(p)$ has the potential to capture both support- and graph-based variation, depending on whether $V$ is calculated relative to $\hat{S}$, which will include support-based effects, or $\bar{S}$, which will not include support-based effects.

## VIII. ASSEMBLING THE PIECES: AN EXPLICIT PRESCRIPTION FOR TDMI ANALYSIS AND INTERPRETATION FOR A POPULATION OF TIME SERIES FOR A FIXED TIME SEPARATION $\delta t$

The interpretation of the TDMI and entropy for a complex, diversely measured population can be split into three broad steps: (i) performing a preliminary interpretation of $\bar{I}(\delta t)$ and $\hat{I}(\delta t)$; (ii) performing an interpretation of $\delta I(\delta t)$ or $\hat{I}(\delta t)$ for the population; and (iii) understanding the make-up of the data explicitly used to estimate the PDFs, yielding an understanding of what proportion of the population as used in the calculation. All the TDMI quantities used for the TDMI-based analysis

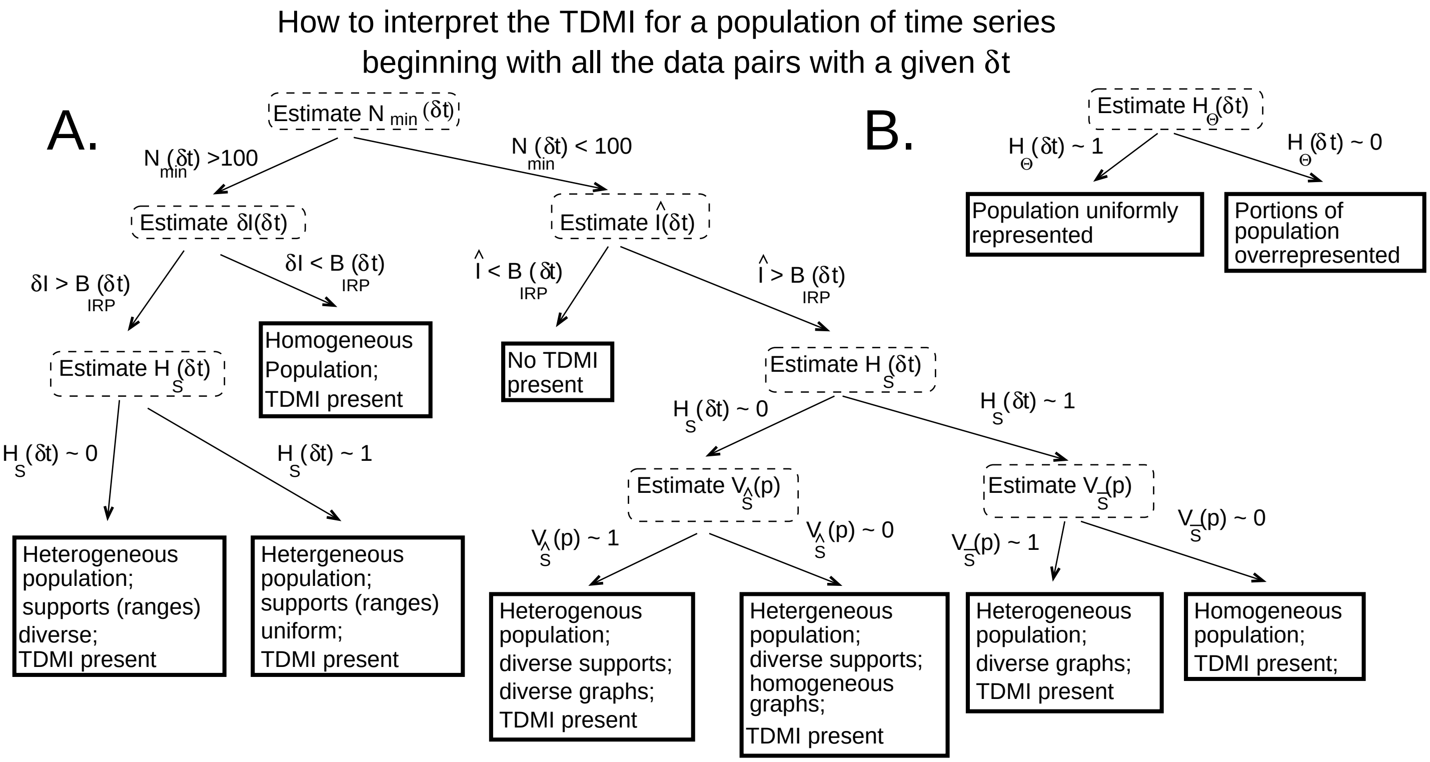
How to interpret the TDMI for a population of time series beginning with all the data pairs with a given δt
A.
Estimate N min (δt)
N min (δt) >100
N min (δt) < 100
Estimate δI(δt)
Estimate Î(δt)
δI > B IRP (δt)
δI < B IRP (δt)
Î < B IRP (δt)
Î > B IRP (δt)
Estimate H S (δt)
Homogeneous Population; TDMI present
No TDMI present
Estimate H S (δt)
H S (δt) ~ 0
H S (δt) ~ 1
H S (δt) ~ 0
H S (δt) ~ 1
Heterogeneous population; supports (ranges) diverse; TDMI present
Hetergeneous population; supports (ranges) uniform; TDMI present
Estimate V Ŝ (p)
Estimate V S̄ (p)
V Ŝ (p) ~ 1
V Ŝ (p) ~ 0
V S̄ (p) ~ 1
V S̄ (p) ~ 0
Heterogenous population; diverse supports; diverse graphs; TDMI present
Hetergeneous population; diverse supports; homogeneous graphs; TDMI present
Heterogeneous population; diverse graphs; TDMI present
Homogeneous population; TDMI present;
B.
Estimate H Θ (δt)
H Θ (δt) ~ 1
H Θ (δt) ~ 0
Population uniformly represented
Portions of population overrepresented

FIG. 2: The graphical schematic for the TDMI analysis of a population.

are shown in table II, a graphical schematic for applying this infrastructure is shown in Fig. 2, and a detailed algorithmic schematic for applying the TDMI infrastructure to a population is depicted via pseudocode in appendix A 3.

### A. Step one: determining the computability of $\bar{I}(\delta t)$

To begin, one must determine whether $\bar{I}(\delta t)$ and $\hat{I}(\delta t)$ are calculable for a given (or set of) $\delta t$(s). In general, to estimate $\bar{I}(\delta t)$ *every representative individual* must (under most circumstances) have at least 100 *pairs of points* available for the TDMI calculation [19]. Similarly, to estimate $\hat{I}(\delta t)$ there must be at least 100 pairs of points *gathered over the entire population*—this is why $\hat{I}(\delta t)$ is so useful in the context of a population.

Assuming that $\bar{I}(\delta t)$ is calculable, because the calculation of $I$ for an individual *is independent of the support of the distribution*, the variance in the distribution of $\bar{I}(\delta t)$ is due to differences in the *graphs* of the PDFs representing each patient at a given $\delta t$. Further, because $\bar{I}(\delta t)$ is made of individuals who have been averaged, the interpretation of the statistical moments of $\bar{I}(\delta t)$ (i.e., the mean, variance, etc), is a scientific problem that depends on the particular circumstances.

The interpretation of $\hat{I}(\delta t)$ is more difficult because $\hat{I}(\delta t)$ can be composed of purely graphical, purely support, and intermixed support and graphical components, Thus, because $\hat{I}(\delta t)$ is a population-dependent quantity where the individual contributions cannot be separated, it will be treated in the next section with $\delta I(\delta t)$.

### B. Step two (A in Fig. 2): interpreting $\delta I(\delta t)$ or $\hat{I}(\delta t)$

Step two has two courses of action depending on whether it is possible to calculate $\bar{I}(\delta t)$ or not: (i) $\bar{I}(\delta t)$ and $\hat{I}(\delta t)$ are calculable and thus $\delta I(\delta t)$ can be computed; and (ii) only $\hat{I}(\delta t)$, $B_{RP}(\delta t)$, and $\mathcal{H}_S(\delta t)$ are calculable (when $\bar{I}(\delta t)$ is calculable, this will always be the case). When $\delta I(\delta t)$ is available, it, as estimated by both a KDE and histogram estimator, is all we need know: the closer $\delta I(\delta t)$ is to zero, the more homogeneous the population is and the more $\hat{I}(\delta t)$ represents a single, statistically singular source and the larger in magnitude $\delta I(\delta t)$ is, the more statistically heterogeneous the population is and the more $\hat{I}(\delta t)$ represents the population. Of course, if the histogram and KDE TDMI estimates differ substantially, it is likely that there are significant small sample size effects present in $\bar{I}(\delta t)$, and this needs to be taken into consideration when interpreting $\delta I(\delta t)$, $\bar{I}(\delta t)$ and $\hat{I}(\delta t)$. Moreover, in this circumstance, calculation of either $B_{RP}(\delta t) = |B_{IRP}(\delta t) - B_{PRP}(\delta t)|$ or $\mathcal{H}_S(\delta t)$ can be used to further qualify the small sample size effects on the variation in the supports versus the graphs. Finally, when $\delta I(\delta t)$ is positive, and $\mathcal{H}_S(\delta t)$ shows no diversity

| TDMI-based analysis quantities | | |
|---|---|---|
| Quantity | What it signifies | What it quantifies |
| $\bar{I}(\delta t)$ | population averaged TDMI | quantifies average TDMI of a population |
| $\hat{I}(\delta t)$ | aggregated population TDMI | quantifies TDMI of an aggregated population |
| $\hat{\mathcal{I}}(\delta t)$ | aggregated population calculated relative to the abstract support $\hat{\mathcal{S}}$ | support independent TDMI of an aggregated population |
| $\delta I(\delta t)$ | $\|\hat{I}(\delta t) - \bar{I}(\delta t)\|$; difference between the average and aggregate TDMI | $\sim 0$ implies homogeneity, $<$ 0 implies heterogeneity |
| $B_E(\delta t)$ | PDF estimator bias; usually $B_E(\delta t) \sim B_{PRP}(\delta t)$; $B_E(\delta t)$ can be estimated in a variety of ways | the number above which the $I$ is considered to be positive |
| $\bar{B}_{IRP}(\delta t)$ | individual permutation bias averaged over a population | bias estimate that preserves information about the relative ranges of individuals |
| $\hat{B}_{IRP}(\delta t)$ | individual permutation bias | bias estimate that preserves information about the relative ranges of individuals |
| $\hat{B}_{PRP}(\delta t)$ | population permutation bias | bias estimate that destroys information about the relative ranges of individuals |
| $\mathcal{H}_S(\delta t)$ | $\frac{\|\hat{B}_{IRP}(\delta t) - \hat{I}(\delta t)\|}{\hat{I}(\delta t)}$; quantifies diversity of supports | $\sim$ 1 implies homogeneous supports; $\sim$ 0 implies diverse supports |
| $B_{RP}(\delta t)$ | $\|\hat{B}_{PRP}(\delta t) - \hat{B}_{IRP}(\delta t)\|$; quantifies diversity of supports; quantifies cardinality of individual data sets | $\sim \hat{B}_{IRP}(\delta t)$ can imply diverse supports or cardinality per-element data sets; $\sim$ 0 can imply homogeneity in supports |
| $\delta G(\delta t)$ | *difference in the difference* between how population diversity renders in $\bar{I}$ and $\hat{I}(\delta t)$ | $>$ 0 implies population diversity |
| $\delta\rho(\delta t)$ | $\| \int_{\bar{\mathcal{S}}} p_1(\bar{\mathcal{S}}) - \int_{\hat{S}} p_1(\hat{S})\|$; quantifies diversity in supports | $>$ 0 implies population diversity. |
| $H_\Theta(\delta t)$ | how representative the population used to estimate $I$ at $\delta t$ is of the time-independent (e.g., the entire) population | $\sim$ 0 implies the entire population is well represented; $\sim$ 1 implies portions of the population are overrepresented |
| $N_{min}(\delta t)$ | minimum number of *pairs* of points contributed by any one individual | a lower bound on the representation of an individual; $1/N_{min}(\delta t)$ is a rough estimate of $B_E(\delta t)$ for the individual with the fewest pairs |

TABLE II: Summary of all the TDMI-based metrics used to interpret the TDMI and determine the population composition.

due to the supports, then all the diversity in the population is due to the graph-based diversity.

When $\bar{I}(\delta t)$ is not calculable, one is left with only $\hat{I}(\delta t)$, $\hat{\mathcal{I}}(\delta t)$, and $B_{RP}(\delta t)$ or $\mathcal{H}(\delta t)$. In this case, one can still use $B_{RP}(\delta t)$ or $\mathcal{H}(\delta t)$ to detect the homo- or heterogeneity in the supports. If there is no support-based variation then pure graph-based heterogeneity maybe be difficult to determine; in this circumstance we recommend using a non-TDMI metric such as $V_S(p)$, which will have greater statistical power while sacrificing temporal dependence, to help determine the graphical composition of the population. In general, if there is support-based variation, it will likely be difficult to separate support-based, versus graph-based, contributions; it will be even more difficult to specify the *proportion* of diversity contributed by the support- versus graph-based effects.

### C. Step three (B in Fig. 2): Assessing population representation

Finally, it is extremely important to understand what portions of the population *actually* have points in a given $\delta t$ bin. Recall that the make-up of the population used to estimate $I$ at a specific $\delta t$ is a concern because of the filtering effect (c.f., section IV C); specifically, it is possible to have entire portions of the population excluded from the data set as well has a highly nonuniform distribution of the population represented in the data set used to estimate the PDFs. Written differently, it is important to always remember that $\delta I$ is always calculated relative to a *fixed* $\delta t$ which will have a particular bin population — when studying the evolution of $I$ as $\delta t$ is varied, *the representative population can change as* $\delta t$ *changes.* Thus, it is important to at least calculate $H_\Theta(\delta t)$ or an $H_\Theta$-like quantity to verify what proportion of the population is being included in the PDF estimate. Moreover, we also find it convenient to keep track of the minimum (and sometimes maximum) number of pairs of points contributed by an element represented in the data set used to estimate the PDFs; we denote this number by $N_{min}(\delta t)$ as a measure of the *least* representative individual.

## IX. QUANTITATIVE EXAMPLES FOR TDMI INTERPRETATION AND POPULATION HOMOGENEITY EVALUATION

### A. Simulated data examples: the quadratic map and the Gauss map

To explicitly demonstrate how to interpret $\bar{I}$ and $\hat{I}$ in the presence of a diverse population in a variety of circumstances, consider two sources of simulated data, the quadratic map

$$x_{t+1} = f(x_t) = ax_t(1 - x_t) \tag{48}$$

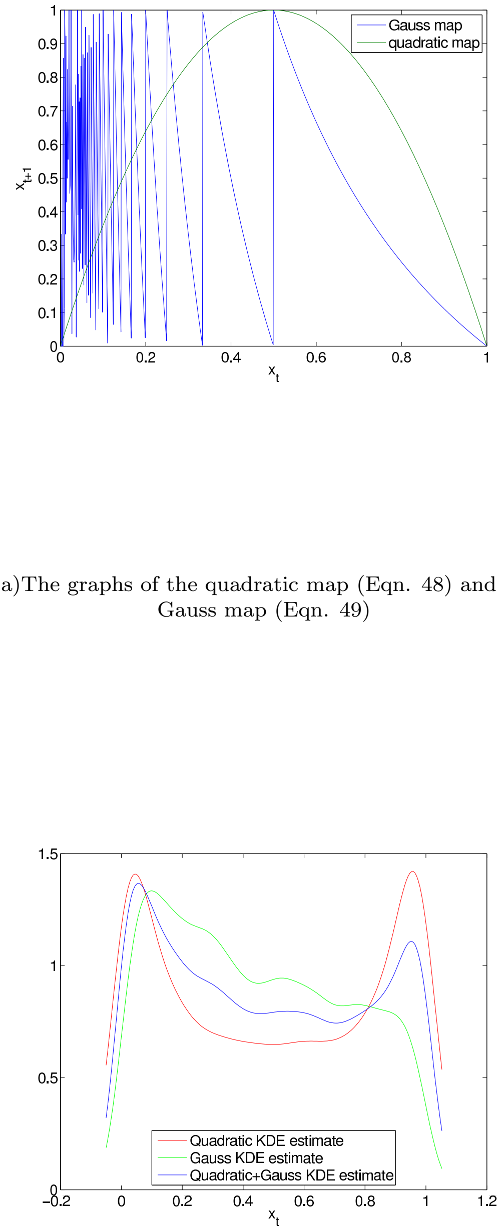

(a)The graphs of the quadratic map (Eqn. 48) and the Gauss map (Eqn. 49)

(b)KDE of the invariant density (PDF of the orbit) for the quadratic map, Gauss map, and the sum of the quadratic and Gauss maps

FIG. 3: The graphs of the quadratic map (Eqn. 48) and the Gauss map (Eqn. 49) — note the significant difference between the graphs of the mappings, and invariant density (PDF of the orbit) for the quadratic map, Gauss map, and the sum of the quadratic and Gauss maps — note the significant differences between the relative $p$'s.

where $a$ is set to 4 and the Gauss map

$$x_{t+1} = g(x_t) = \frac{1}{x_t} \mod 1 \tag{49}$$

These sources were chosen because their statistical structures are well understood [23] [24] [2], they are chaotic, they are both 1-dimensional maps defined over the unit interval (meaning, they have the same support), and they have relatively different invariant densities. Figure 3 shows the the graphs of the quadratic and Gauss maps, their individual invariant densities (PDFs of the orbit), and the sum of their invariant densities. Thus, in this context, the difference between $p_f$ and $p_g$, $\epsilon(x)$, is both large enough such that the $G$'s will be non-zero and is non-uniform over the domain or nonlinearly dependent on $x$. The data sets we will use, based on the maps above, include:

**Data set 1** *Quadratic map time-series with* 1000 *points; this is one of the data sets meant as a baseline from which all the other cases can be compared.*

**Data set 2** *Gauss map time-series with* 1000 *points; this is one of the data sets meant as a baseline from which all the other cases can be compared.*

**Data set 3** *Data sets* 1 *and* 2 *concatenated into a single data set with* 2000 *data points; this data set is used primarily to test the effects of differing PDFs within a population on $\iota$, $G$, and thus, $\bar{I}$ versus $\hat{I}$.*

**Data set 4** 50 *independent, concatenated quadratic map time-series with* 20 *points each totally* 1000 *points; this data set is meant to highlight the effect of the estimator bias when calculating $\bar{I}$ versus $\hat{I}$.*

**Data set 5** 10 *independent, concatenated quadratic map time-series with* 100 *points each totaling* 1000 *points; this data set is meant to form a baseline for data set* 6*.*

**Data set 6** 10 *independent, concatenated quadratic map time-series with* 100 *points with* disjoint *supports with increasing means totaling* 1000 *points; this data set is used to demonstrate the effect of diverse supports amongst the population where the PDFs are identical on $\iota$, $G$, $B$, and thus $\bar{I}$ versus $\hat{I}$.*

Each data set will be denoted by $D_i$ where $i$ is the indexed label of the respective data set.

Finally, to save space, we will demonstrate the TDMI and non-TDMI-based computations on all the simulated data sets at one time. We will adhere to the algorithm shown in Fig. 2 when analyzing the real data sets.

### *1. TDMI-based analysis of the simulated data*

| TDMI-based quantities | | | | | | | | | |
|---|---|---|---|---|---|---|---|---|---|
| Source | $\bar{I}(\tau=1)$ | $\hat{I}(\tau=1)$ | $\bar{B}_{IRP}(\tau=1)$ | $\hat{B}_{PRP}$ | $\hat{B}_{IRP}(\tau=1)$ | $B_{RP}(\tau=1)$ | $\mathcal{H}_S(\tau=1)$ | $\delta\rho(\tau=1)$ | $\delta G(\tau=1)$ | $\delta I(\tau=1)$ |
| $D_1$ | 0.72 | — | 0.008 | 0.008 | 0.008 | 0 | 0.99 | 0 | 0 | 0 |
| $D_2$ | 0.31 | — | 0.012 | 0.012 | 0.012 | 0 | 0.96 | 0 | 0 | 0 |
| $D_3$ | 0.52 | 0.37 | 0.01 | 0.008 | 0.007 | 0.001 | 0.98 | 0 | 0.15 | 0.15 |
| $D_4$ | $0.34 \pm 0.07$ | 0.71 | $0.18 \pm 0.03$ | 0.013 | 0.011 | 0.002 | 0.98 | 0 | $\delta I$ | $0.37 \pm 0.07$ |
| $D_5$ | $0.48 \pm 0.01$ | 0.71 | $0.04 \pm 0.01$ | 0.006 | 0.007 | 0.001 | 0.99 | 0 | $\delta I$ | $0.24 \pm 0.01$ |
| $D_6$ | $0.48 \pm 0.01$ | 1.12 | $0.04 \pm 0.01$ | 1.12 | 0.011 | 1.11 | 0 | unknown | unknown | $0.55 \pm 0.01$ |

TABLE III: TDMI results and homogeneity metrics for the simulated data sets one through six.

**Base cases: testing the TDMI-based metrics on individuals**—In table III one can see that both the quadratic and Gauss maps have distinctly different $I(\tau = 1)$ values. Note that the Gauss map has a faster decay in correlations; for both maps, all correlations in time decay by $\tau = 6$. Further notice that all bias estimation schemes are essentially identical as expected. This also implies that support-variation detecting quantities such as $\mathcal{H}_S$ register no variation in supports.

**Support dependent, *graph independent* analysis**—To see how diverse supports are rendered, consider the contrast between $D_5$ and $D_6$, whose only difference is in the *location* of the supports. Both of the support-based TDMI based metrics, $B_{RP}$ and $\mathcal{H}_S$, produced dramatic representations of the disjoint nature of the supports of data set six (c.f., table III). Notably, the difference between both $B_{RP}$ and $\mathcal{H}_S$ on $D_5$ and $D_6$ are near their respective maxima.

**Graph dependent, support *independent* analysis**—Data set three, the quadratic-Gauss aggregated data set, has homogeneity in support in all support-based metrics as can be seen in table III. In particular, both $\mathcal{H}_S$ and all the random permutation bias estimates are totally unaffected by the existence of $\bar{\epsilon}$ or $\hat{\epsilon} \neq 0$. Furthermore, $\delta I \neq 0$, meaning that the population averaged TDMI and the TDMI of the aggregated population were different. In particular, $\bar{I} > \hat{I}$, thus leading to the conclusion that $\bar{G} > \hat{G}$, which is not surprising given that when the $\bar{\epsilon}_i = \hat{\epsilon}_i$ for all $i$, it is reasonable that the $\epsilon$'s register greater though the sum than the aggregate. In any event, all the TDMI based metrics registered the diversity in the population of PDFs.

**Support dependent graph-based analysis**—To begin to see how support and graph effects intermix, consider $\hat{I}$ for a data set identical to $D_6$ except where the quadratic data has been replaced with uniform random numbers, thus yielding data with purely population location information; denote this data set as $D'_6$. Now, $\hat{I}(D'_6) \approx 1.16 \pm 0.01$, thus comparing $\hat{I}(D_6)$ to $\hat{I}(D'_6)$, we notice that the presence of intra-agent time-based correlation *decreases the population scale TDMI* by a small but measurable amount — here $|\hat{I}(D_6) - \hat{I}(D'_6)| \approx 0.04$. Therefore, while nearly all the intra-agent TDMI is subsumed by the inter-agent TDMI, when there is a presence of both strong intra-agent information as well as strong inter-agent information (i.e., highly disjoint supports), $\hat{I}$ will contain *both* intra-agent and inter-agent components.

What the example in the previous paragraph shows is that deducing the contribution of the intra-agent and inter-agent components to $\hat{I}$ will in many cases, be non-trivial. Nevertheless, the use of metrics that detail the PDF variation can sometimes aid in the interpretation of $\hat{I}$. First, considering how the heuristic metrics of PDF variation render the variation in PDFs, note that both the super sensitive $H_{RA}$ and more robust, less sensitive $V(p)$, for $D_6$, are about double their values for $D_5$, even though $D_5$ will yield considerably noisier PDF estimates. Similarly, the TDMI metrics for PDF variation also render population diversity; $\delta I$ for $D_6$ is more than twice $\delta I$ for $D_5$. However, $\delta I$ for $D_6$ has a slightly more complicated interpretation. In particular, while $\delta I$ represents the difference between the population and the individual TDMI, there is likely a non-trivial component of $\bar{I}$ that is a function of sample size. Thus, $\delta I$ is not purely the difference between the individual and the population TDMI for unlimited data as it was for $D_3$. Nevertheless, because $\bar{I} \gg B_E(D_6)$, and $\delta I \gg B_E(D_6)$ we know that $\hat{I}$ has components of both individual and population scale TDMI. In fact, considering $|\hat{I}(D_5) - \hat{I}(D_6)| \approx 0.41$ versus $|\hat{I}(D_5) - \hat{I}(D'_6)| \approx 0.44$, one can see that for this case, the TDMI whose source is in the population dominates; presumably if the supports for $D_6$ were nearly overlapping instead of disjoint, $|\hat{I}(D_5) - \hat{I}(D_6)|$ would be much closer to zero. While it is unusual to be able to compare identical, stationary systems with differing supports, this analysis does suggest that calculating $\hat{I}$ for the raw data and for the data with normalized supports may be useful for determining the proportion of $\hat{I}$ that is due the diversity of the supports.

### 2. *Non-TDMI-based analysis of the simulated data*

**Base cases: testing the non-TDMI metrics on individuals**—Begin by considering $D_1$ and $D_2$, both of which represent only a single individual. Both cases are well defined in $p$ (c.f., Fig. 3), and have supports whose lengths, $|S|$, and boundaries, $s_{min}$, $s_{max}$, are well resolved and within their expected ranges (c.f., table IV).

**Support dependent, *graph independent* analysis**—To see how variations in the supports are rendered, consider the contrast between $D_5$ and $D_6$, whose only difference is in the *location* of the supports. Focusing on $D_6$, variation in the support shows up in the heuristic metrics $s_{min}$, $s_{max}$, $|S|$, and especially in the variance of $s_{min}$ and $s_{max}$.

**Graph dependent, support *independent* analysis**—Data set three, the quadratic-Gauss aggregated data set, has homogeneity in support in all support-based metrics as can be seen in tables IV as expected. In contrast, both of the heuristic metrics designed to detect variation in PDFs registered as non-zero, meaning they detected variation in the PDFs. Moreover, the $l_1$-like diagnostic, $H_{RA}$ was more sensitive than the variance based metric, $V_{\bar{S}}(p)$, as expected.

**Support dependent graph-based analysis**—None of the examples mix graph and support effects simultaneously by design.

### 3. *Quantifying small sample-size effects*

To form a baseline of small sample size effects for both real data applications and the support-based effects, we focus on comparing and constraining results for $D_4$ and $D_5$, the quadratic map data sets with 50 sets of 20 points, and 10 sets of 100 points.

**Small sample size effects on non-TDMI-based support analysis metrics**—The heuristic metrics of support diversity show homogeneity in support. However, it is important to note that the invariant density of the quadratic map has most of its mass at the end points, and thus may represent the best case scenario for support based metrics on small data sets.

**Small sample size effects on TDMI-based support analysis metrics**—The TDMI based metrics of support diversity show homogeneity of support, although the individual-wise random perturbation for the random case ($B_{IRP}$) is rather high, especially for the 20 point data sets, as one might expect. However, we hypothesize that the primary reason why $B_{IRP}$ is so high for the 20 point data sets is that, upon randomly permuting any data set, the average $\tau$ will be the length of the data set over 3, in this case, $\frac{20}{3} < 7$. Thus, for very short data sets, it can be difficult to approximate the estimator bias using only the random permutation method [19].

**Small sample size effects on non-TDMI-based graph analysis metrics**—In contrast to the support-based effects, the heuristic-based PDF variability metrics register *substantial* diversity among the PDFs $D_4$ and $D_5$, effects that are entirely a function of small sample sizes. These results are not surprising given that there will be great variance in the PDF estimate of a quadratic time-series with only 20 points.

**Small sample size effects on TDMI-based graph analysis metrics**—The small sample size situation highlights both the difference between $\bar{I}$ and $\hat{I}$ and also displays the motivation for why one would want to estimate $\hat{I}$. The *average* based TDMI results for both $D_4$ and $D_5$ *do not* approximate the 1000 point analogs; and moreover, the addition of more *sets* of data with similar lengths will not help the $\bar{I}$ to converge to the higher point analog but rather decrease the variance in the mean $\bar{I}$ value. Thus, the desired meaning of $\bar{I}$ is, in a sense, a precision/accuracy type problem; adding more 20 point data sets will make the estimate of $\bar{I}$ more precise, but not necessarily more accurate. That said, accuracy is always defined relative to a target; there is likely less TDMI in the 20 point data set because there is considerably less time-based information in a 20 or 100 point data set than in a 1000 point data set. Therefore, while adding more data sets will not aid in convergence to the infinite point analog, the infinite point analog may not be right target to be aiming for with 20 point data sets. In contrast, the *aggregated* data sets produce a TDMI equivalent to the 1000 point analog, thus inducing a $\delta I$. Moreover, adding points to the aggregated data set will help with convergence to $I(\tau = 1)$ for infinitely long data strings.

**Interpreting $\delta I$ when individual elements have few pairs of points**—The existence of $\delta I$ for $D_4$ and $D_5$ introduces a form of divergence from $I(\tau = 1, N = \infty)$ that is not quite a bias (either estimator or non-estimator); the "true" amount of information in a data string of length 20 is fundamentally different from the "true" amount of information in a data string of length $N = \infty$ — thus $\delta I$ can also exist due to finite sample size effects. Or, said more quantitatively, $\bar{I}$, even for an unlimited collection of 100 point data strings, will never be within estimator bias or any other kind of bias, of $I(\tau = 1, N = \infty)$ because $I(\tau = 1, N = \infty) \sim 0.72$ while $I(\tau = 1, N = 20) \approx 0.48 \pm 0.1$. What this means for $\hat{I}$ is that, unless the aggregated data sets are homogeneous enough in their time-dependent correlation structure, $\hat{I}$ will likely represent *population distribution* information, as $\bar{I}$ would represent the upper bound on time-correlation based information present in each data string. Often the composition of most real world data streams can be difficult to infer; and moreover, it can be a non-trivial problem to discern whether $\bar{I}$ or $\hat{I}$ most faithfully represent a population or individual effects. For instance, in Ref. [25], the authors claim both the presence of time-correlation information and population-based time-correlation being simultaneously present. Usually a careful analysis of the population composition of the $\delta t$ bins

| non-TDMI-based population diversity metrics | | | | | | | |
|---|---|---|---|---|---|---|---|
| Source | $H(\bar{x})$ | $\mathrm{Var}(n_i)$ | $s_{min} \pm V_{s_{min}}$ | $s_{max} \pm V_{s_{max}}$ | $\lvert S\rvert \pm V_{\lvert S\rvert}$ | $H_{RA}$ | $V_{\bar{\mathcal{S}}}(p)$ |
| D1 | 0 | 0 | 0.0001 | 0.999 | 0.9989 | 0 | 0 |
| D2 | 0 | 0 | 0.0002 | 0.9998 | 0.9997 | 0 | 0 |
| D3 | 0 | 0 | $0.0002 \pm 0.0003$ | $0.9989 \pm 0.0015$ | $0.9987 \pm 0.0018$ | 0.16 | 0.09 |
| D4 | 0 | 0 | $0.02 \pm 0.02$ | $0.996 \pm 0.006$ | $0.98 \pm 0.03$ | 0.9 | 0.39 |
| D5 | 0 | 0 | $0.001 \pm 0.002$ | $0.9997 \pm 0.0006$ | $0.998 \pm 0.003$ | 0.37 | 0.13 |
| D6 | 0 | 0 | $5.5 \pm 3$ | $6.5 \pm 3$ | $0.997 \pm 0.004$ | 0.68 | 0.32 |

TABLE IV: Heuristic homogeneity metrics for the simulated data sets one though six.

will help rectify this difficulty.

### B. Real data examples: glucose values for 100 densely sampled individuals versus 20,000 random individuals

We now move on to applying the insights and techniques of the previous sections to real data. In particular, we will consider two data sets that contain different populations of patients from the CUMC data repository. More specifically, the data sets include:

**Data set 7** *a collection of the* 100 *patients with the most glucose measurements in the database, ranging from* $\sim 4000$ *to* $\sim 1500$ *measurements per patient;*

**Data set 8** *a collection of* 20,000 *random patients with at least* 2 *glucose measurements from among the* 800,000 *patients with glucose values.*

To visualize these populations, consider Fig. 4 where the normalized PDFs for each individual for each population and the PDF of the overall populations are plotted. While the population-wide PDFs, shown in Fig. 4(c) are not wildly different, the relative diversity within the two populations, as shown in Figs. 4(a) and 4(b), is dramatic. The motivation for choosing $D_7$ is that, for this set, because each patient has *at least* 1000 lab values, both $\bar{I}$ and $\hat{I}$ are calculable. Moreover, the authors hypothesize that patients with so many glucose values are more likely to represent a more homogeneous population compared with the population at large. Given the makeup of $D_7$, $D_8$ represents not only a contrast to $D_7$ in that $D_8$ is a snapshot of the entire population, but $D_8$ also represents a pathologically difficult situation data-wise — very few patients have more than 100 glucose values, and the set of possible causes for the existence of a glucose measurement is extremely large (or broad). Thus, not only will $\bar{I}$ be difficult to calculate for $D_8$ (most patients won't have enough data to generate a PDF estimate), but there is likely tremendous and differing diversity amongst the patients actually included in the estimates of $\bar{I}$ and $\hat{I}$.

Finally, note that in contrast to the previous analysis of simulated data, we will present the TDMI results first, followed by an analysis using the non-TDMI metrics to verify the TDMI results. The point of this ordering is to demonstrate the TDMI infrastructure without hindsight knowledge.

#### 1. TDMI-based analysis for data set 7, the well measured population

**Analysis of the $\delta t = 6$ hrs time separation using the algorithm in Fig. 2**—First, considering table V, note that for $D_7$ with a $\delta t = 6$hrs, we are able to estimate $\bar{I}$, and thus $\delta I$ because $N_{min}(6hrs) > 100$. Next, note that $\delta I(6hrs)$ is considerably above $B_{IRP}(6hrs)$, meaning that the population is on the time-scale of 6 hours is heterogeneous. Moreover, both $\bar{I}(6hrs)$ and $\hat{I}(6hrs)$ are greater than zero, meaning that there is TDMI present in individuals and the aggregated population. To determine the nature of heterogeneity, further consider the support-based metric; $\mathcal{H}_S(6hrs) \sim 1$ points to the population having uniformity in supports or ranges ($B_{RP}(6hrs) \approx B_{IRP}(6hrs)$ which corroborates this conclusion). Finally, the entire population is reasonably represented for $\delta t = 6hrs$ as confirmed by the fact that $N_{min}(6hrs) \sim 500$ and $H_{\Theta}(6hrs) \gg 0$. Thus, the concluding interpretation is as follows: the population is heterogeneous on the $\delta t = 6$hrs time scale; the heterogeneity in the population is in the graphs not the supports (or the normalizations; there is diverse but present temporal correlation among the population (i.e., the TDMI is not due to the population aggregation, but exists because of the individuals); and the entire population is well represented in the TDMI-based quantities.

**Analysis of the $\delta t = 24$ hrs time separation using the algorithm in Fig. 2**—First, considering table VI, note that for $D_7$ with a $\delta t = 24$hrs, we are able to estimate $\bar{I}$, and thus $\delta I$ because $N_{min}(24hrs) > 100$.

| TDMI-based quantities for the $\delta t = 6$ hrs time separation | | | | | | | | | | |
|---|---|---|---|---|---|---|---|---|---|---|
| Source | $\bar{I}$ | $\hat{I}$ | $\delta I$ | $\bar{B}_{PRP}$ | $\hat{B}_{IRP}$ | $\hat{B}_{PRP}$ | $B_{RP}$ | $\mathcal{H}_S$ | $H_\Theta$ | $N_{min}$ |
| $D_7$ | $0.64 \pm 0.03$ | 0.22 | $0.42 \pm 0.03$ | $0.02 \pm 0.01$ | $0.02 \pm 0.005$ | $0.001 \pm 0.0005$ | $\sim \hat{B}_{IRP}$ | $1 \pm 0.0005$ | 0.31 | 470 |
| $D_8$ | $0.29 \pm 0.16$ | 0.38 | $0.09 \pm 0.37$ | $0.2 \pm 0.2$ | $0.08 \pm 0.005$ | $0.006 \pm 0.0005$ | $\sim \hat{B}_{IRP}$ | $1 \pm 0.02$ | 0.003 | 1 |

TABLE V: TDMI results and homogeneity metrics for the real patient data sets seven and eight; note all $\delta t$ times are in hours.

| TDMI-based quantities for the $\delta t = 24$ hrs time separation | | | | | | | | | | |
|---|---|---|---|---|---|---|---|---|---|---|
| Source | $\bar{I}$ | $\hat{I}$ | $\delta I$ | $\bar{B}_{PRP}$ | $\hat{B}_{IRP}$ | $\hat{B}_{PRP}$ | $B_{RP}$ | $\mathcal{H}_S$ | $H_\Theta$ | $N_{min}$ |
| $D_7$ | $0.093 \pm 0.06$ | 0.077 | $0.016 \pm 0.06$ | $0.02 \pm 0.01$ | $0.02 \pm 0.005$ | $0.001 \pm 0.0005$ | $\sim \hat{B}_{IRP}$ | $0.99 \pm 0.01$ | 0.33 | 479 |
| $D_8$ | $0.21 \pm 0.15$ | 0.17 | $0.04 \pm 0.15$ | $0.3 \pm 0.2$ | $0.07 \pm 0.01$ | $0.005 \pm 0.001$ | $\sim \hat{B}_{IRP}$ | $0.97 \pm 0.001$ | 0.005 | 1 |

TABLE VI: TDMI results and homogeneity metrics for the real patient data sets seven and eight; note all $\delta t$ times are in hours.

| time independent TDMI-based quantities | | |
|---|---|---|
| Source | $\bar{h}$ | $\hat{h}$ |
| $D_7$ | $1.39 \pm 0.07$ | 2.12 |
| $D_8$ | $0.8 \pm 0.22$ | 2.05 |

TABLE VII: Time *independent* TDMI results for the real patient data sets seven and eight..

Next, note that $\delta I(24hrs)$ is within the error bars of zero (e.g., below $B_{IRP}(24hrs)$), meaning that the population is on the time-scale of 24 hours is *homogeneous*. Moreover, both $\bar{I}(24hrs)$ and $\hat{I}(24hrs)$ are greater than zero, meaning that there is TDMI present in individuals and the aggregated population. To determine the nature of heterogeneity, further consider the support-based metric; $\mathcal{H}_S(24hrs) \sim 1$ points to the population having uniformity in supports or ranges ($B_{RP}(24hrs) \approx B_{IRP}(24hrs)$ which corroborates this conclusion). Finally, the entire population is reasonably represented for $\delta t = 24hrs$ as confirmed by the fact that $N_{min}(24hrs)$ 500 and $H_\Theta(24hrs) \gg 0$. Thus, the concluding interpretation is as follows: the population is homogeneous on the $\delta t = 24$hrs time scale; there is present temporal correlation among the population (i.e., the TDMI is not due to the population aggregation, but exists because of the individuals); and the entire population is well represented in the TDMI-based quantities.

**Analysis independent of time**—Considering the entropy calculations in table VII, $D_7$ renders some heterogeneity because the difference between $\bar{h}$ and $\hat{h}$ is nonzero. Nevertheless, as we will see for $D_8$, an entropy difference of 0.73, which is about half the magnitude of $\bar{h}$, would argue that the *static* information theoretic interpretation of the population is of relative homogeneity.

**Sample size issues**—There were no sample size issues with respect to either $\delta t$ time separations studied; in both cases, $N_{min}$ was well over 100, and thus all PDFs and their respective biases could be accurately estimated. In fact, careful analysis of the population make-up in each $\delta t$ between 6hrs and 56hrs revealed that the proportionally of each individual remained relatively constant. Finally Fig. 6, where both the TDMI estimated using both KDE and histogram estimation schemes are shown, confirms the lack of any small sample size effects because both estimation schemes are essentially equal.

### 2. *non-TDMI-based analysis for data set 7, the well measured population*

**Non-TDMI support-based analysis**—To verify the TDMI-based results, begin by observing that heuristic metric that quantifies variation in the supports, $H(\bar{X}) \approx 1$, which is considered small. Thus, while there is some diversity among how the patients were measured, variation how patients are measured is small. This claim is also justified by the fact that the variance in the number of points contributed, per patient, to the $\delta t = 6hrs$ bin, $Var(n_i)$, is small. Finally, the variance in $s_{min}$, $s_{max}$ and $|S|$ is small compared to the respective values (c.f., Fig. 5(a)). Because these are *time-independent* measures of the support, and because adding the temporal aspect of the analysis only makes the data set smaller, it is likely that the TDMI analysis of the homogeneity of support are correct.

**Non-TDMI graph-based analysis**—The most sensitive PDF variation metric, $H_{RA}$ points to a relatively diverse population, while the less sensitive PDF variation metric $V_{\bar{S}}(p)$, based on the standard deviation of the *distribution* of PDFs, points to a relatively homogeneous, yet not totally homogeneous population. Figure 5 confirms this analysis visually. The maxima minus

| non-TDMI-based analysis metrics | | | | | | | |
|---|---|---|---|---|---|---|---|
| Source | $H(\bar{x})$ | Var$(n_i)$ | $s_{min} \pm V_{s_{min}}$ | $s_{max} \pm V_{s_{max}}$ | $\lvert S\rvert \pm V_{\lvert S\rvert}$ | $H_{RA}$ | $V_{\bar{\mathcal{S}}}(p)$ |
| $D_7$ | 1.042 | 463.7 | $29.7 \pm 10.7$ | $445.0 \pm 58.8$ | $415.4 \pm 62.7$ | 0.898 | 0.432 |
| $D_8$ | 30 | 55 | $84 \pm 35$ | $150 \pm 122$ | $66 \pm 125$ | 1 | 0.90 |

TABLE VIII: Heuristic homogeneity metrics for the real patient data sets seven and eight.

the minima, which, when integrated is essentially $H_{RA}$, shown in Fig. 5(b), can be seen to be relatively large, thus making $H_{RA}$ render diversity. In contrast, the variance in the graphs of the PDFs, shown in Fig. 5(c), is seen as relatively small for $D_7$, thus making $V_{\bar{\mathcal{S}}}(p)$ render relative homogeneity. It is important to note, however, that $V_{\bar{\mathcal{S}}}(p)$, which is independent of time, does not detail the fact that the population has diverse predictive information for time periods less than 6 hours; this is an important distinction to make as it implies that prediction can vary with time despite the overall distribution of physiological variables. Finally, both the TDMI and the heuristic analysis conclude that the population is homogeneous in supports and in the long term (i.e., independent of time), the population is homogeneous; this is because $\delta I \sim 0$ for $\delta t > 12$ hrs and $V_{\bar{\mathcal{S}}}(p)$ is small.

### 3. *TDMI-based analysis for data set 8, the random (less well measured) population*

**Analysis of the $\delta t = 6$ hrs time separation using the algorithm in Fig. 2**—First, considering table V, note that for $D_8$ with a $\delta t =$ 6hrs, we are *not* really able estimate $\bar{I}(6hrs)$ because $N_{min}(6hrs) = 1$. To interpret $\hat{I}(6hrs)$, we consider the support-based metric; $\mathcal{H}_S(6hrs) \sim 1$ which points to the population, *which was filtered and has time points separated by 6 hours*, having uniformity in supports or ranges ($B_{RP}(6hrs) \approx B_{IRP}(6hrs)$ which corroborates this conclusion). To give intuition to the graph-based variation, consider $V_{\bar{\mathcal{S}}}(p)$ (table VIII), which implies a somewhat diverse population. Moreover, $V_{\bar{\mathcal{S}}}(p)$ for $D_8$ is *twice that* of $D_7$, implying that the population in $D_8$ is more diverse than that of $D_7$. Moving beyond the algorithm shown in Fig. 2, we did estimate $\bar{I}(6hrs)$ and thus, $\delta I(6hrs)$, only including individuals with enough points to estimate $I$. Based on this restricted version of $\delta I(6hrs)$, the population appears to be homogeneous. Nevertheless, both the restricted $\bar{I}(6hrs)$ and $\hat{I}(6hrs)$ are greater than zero, meaning that there is TDMI present in individuals and the aggregated population. This means that there is an apparent contradiction; the *restricted* $\delta I(6hrs)$ implies a population that is somewhat homogeneous/heterogeneous while $V_{\bar{\mathcal{S}}}(p)$ implies a heterogeneous population. This contradiction is resolved by recalling that $V_{\bar{\mathcal{S}}}(p)$ is calculated on the *entire, non-filtered population* and is *independent of time* and will overestimate graphic diversity, while $\delta I$ is overly restricted and will underestimate diversity. This interpretation will be substantiated further in sections IX B 5 and IX B 6. Finally, the overall population is *poorly* represented for $\delta t = 6hrs$ as confirmed by the fact that $N_{min}(6hrs) = 1$ and $H_{\Theta}(6hrs) \approx 0$. In fact, for $D_8$, we know that 63% of the patients $(12,763)$ have *no points* in the $\delta t = 6hrs$ bin, and only 12% $(2,400)$ of the patients have ten or more points in the $\delta t = 6hrs$ bin. Thus, the concluding interpretation is as follows: the population is homogeneous on the $\delta t =$ 6hrs time scale up to what is resolvable by $\delta I(6hrs)$; the represented population has relatively uniform supports; there is diverse but present temporal correlation among the population (i.e., the TDMI is not due to the population aggregation, but exists because of the individuals); the population has diversity relative to their time-independent graphs, but this graph diversity may not reflect the graph diversity of the represented population (i.e., the population used to estimate the TDMI-based quantities); the overall population of patients is poorly represented in the TDMI-based diagnostics; and finally the overall population of $20,000$ patients is diverse, but the patients that have enough data to estimate the TDMI on time-scales of $\delta t \leq 48hrs$ (i.e., the represented population), which represents a strongly filtered subpopulation, is relatively homogeneous in predictive information *regardless of* $\delta t$.

**Analysis of the $\delta t = 24$ hrs time separation using the algorithm in Fig. 2**—Considering table VI (and later, Fig. 6(b)), the analysis of the TDMI diagnostics for $\delta t =$ 24hrs is essentially identical to $\delta t =$ 6hrs case. Even representative population for both the $\delta t = 6$ and 24hrs bins is essentially identical down to the individual proportional contributions to the aggregated data set. Thus, the key observation here is the difference between $D_7$ and $D_8$; $D_7$ registered heterogeneity at $\delta t =$ 6hrs and homogeneity at $\delta t =$ 24hrs whereas $D_8$ does not render a $\delta t$ dependence in the TDMI-based diagnostics.

**Analysis independent of time**—Considering the entropy calculations in table VII, $D_8$ renders heterogeneity because the difference between $\bar{h}$ and $\hat{h}$ is non-zero. In particular, compared to the entropy differences for $D_7$, the $D_8$ has an entropy difference of $\sim 1.25$, which is substantially *larger* in magnitude than $\bar{h}$. Thus the *static* information theoretic interpretation of the population in $D_8$, which includes all patients (there is not filtering effect), is of heterogeneity.

**Sample size issues**—There are three sample size issues present in the TDMI analysis of $D_8$, the poor representation of the overall population, the inability to estimate $I$ for every representative member of the pop-

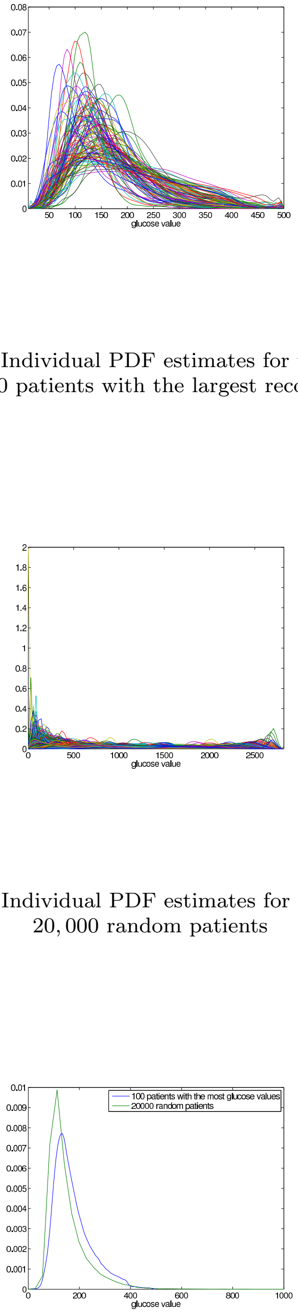

(a)Individual PDF estimates for the 100 patients with the largest record

(b)Individual PDF estimates for the 20, 000 random patients

(c)Aggregated population PDF comparison

FIG. 4: PDFs of glucose measurements for individuals within a population and for a population for two data sets, the 100 patients with the largest records and 20, 000 random patients

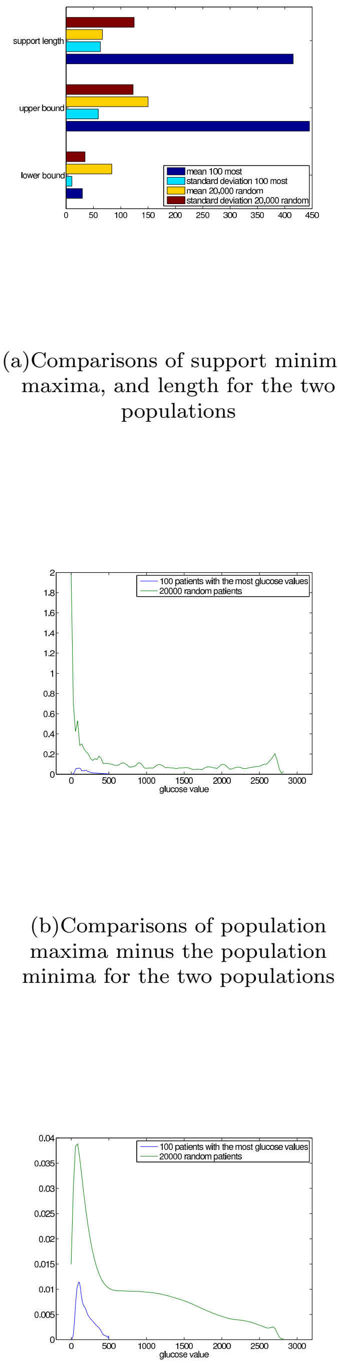

(a)Comparisons of support minima, maxima, and length for the two populations

(b)Comparisons of population maxima minus the population minima for the two populations

(c)Comparisons of the standard deviation of the PDF graphs for the two populations

FIG. 5: Comparisons of the supports, and PDF graph variations for two data sets, the 100 patients with the largest records and 5000 random patients

ulation, and the overall small sample size and bandwidth/normalization issues. The first issue implies that the probability mass used to estimate the PDFs comes from a *very small subset of the population*; e.g., only 12% of the population has 10 or more points in the $\delta t = 6hrs$ bin. Thus, the restricted (i.e., filtered) population is likely substantially more homogeneous than the overall population, and the TDMI analysis cannot be said to represent the overall population. Relative to the second issue, since $N_{min} = 1$ (for both $\delta t = 6$ and 24 hrs), $\bar{I}(\delta t)$ is representative of a smaller population than $\hat{I}(\delta t)$. Finally the third issue, small sample size effects, can be seen in the large difference (about a factor of 2) between the KDE and histogram estimator based TDMI values seen in Fig. 6.

### *4. non-TDMI-based analysis for data set 8, the random (less well measured) population*

**Non-TDMI support-based analysis**—Begin by noticing that there is considerable diversity in how the 20,000 patients are measured, as can be seen in $H(\bar{X}) \approx 30$, which is 30 times larger $H(\bar{X})$ for $D_7$. Considering this in conjunction with $Var(n_i) \approx 50$ for $D_8$, which is much smaller than $Var(n_i)$ for $D_7$, implies that very few of the patients have many points. Said differently, the reason why $Var(n_i)$ is relatively small compared to $H(\bar{X})$ is that $n_i$ is bounded from below by 0 and is never very large for any member of $D_8$. That this is the fact is reflected in variance in $s_{min}$, $s_{max}$ and $|S|$, which is large (on the order of, or greater than) the values of $s_{min}$, $s_{max}$ and $|S|$ respectively (c.f., Fig.5 ). Heuristically this effect can be seen by observing the range of values seen in Fig. 4(b) versus Fig. 4(a) — the population of 20,000 yields a range of glucose values roughly five times that of $D_7$.

**Non-TDMI graph-based analysis**—The most sensitive PDF variation metric, $H_{RA}$ points to a relatively diverse population. In contrast to the results for $D_7$, the less sensitive PDF variation metric $V_{\bar{S}}(p)$, also points to a heterogeneous population; in particular, $V_{\bar{S}}(p)$ is just about twice the $V_{\bar{S}}(p)$ for $D_7$.

### *5. Analysis of the TDMI under variation of $\delta t$*

A central motivation for using the TDMI is to observe how nonlinear correlation evolves in time; however, in the context of a diversely measured population, one must take care to ensure the TDMI signal represents a relatively constant population. Relative to $D_7$ and $D_8$, we know that, for $\delta t$ between 6 and at least 56 hours, the representative population is roughly constant. Figure 6 details the temporal evolution of the TDMI, and with it, exhibits five notable features.

First, both data sets display diurnal peaks in predictability; a full explanation of these peaks, which is dependent the structure of meal times [26]. This is scientifically interesting because it is a signal that can be used to test physiological models, it can be used to distinguish populations, it implies that outside of very local time windows, measurements separated by 24 are more informative than measurements separated by fewer hours, and finally, the diurnal peaks confirm the presence of diurnal cycles in humans that are believed to exist.

Second, relative to $D_7$, the population appears to be *heterogeneous* on time scales of 6 hours and less, and *homogeneous* on time scales longer than 6 hours. This can be seen in Fig. 6(a), where $\delta I(6hrs)$ is relatively large and drops to zero by $\delta t = 12$ hrs. This is an interesting result that we are still working to understand.

Third, by comparing the results for $D_7$ and $D_8$, we can observe a difference in the degree of homogeneity amongst the population. In particular combining the facts that the error bars for $\bar{I}$ are large for $D_8$ compared to $D_7$, $\delta I$ is independent of $\delta t$ for $D_8$, $\delta I$ for $D_8$ is much larger than for $D_7$, and the broad qualitative TDMI signal (i.e., the diurnal peaks) is the same for both $D_7$ and $D_8$, it seems clear that both data sets have somewhat homogeneous populations (i.e., homogeneous enough to resolve a similar signal), but $D_7$ is considerably more homogeneous than $D_8$.

Fourth, considering Fig. 6(b), it is clear that the aggregate TDMI resolves the diurnal peaks considerably better than the average TDMI. This is confirms the usefulness of the aggregate TDMI in the context of a complex, diversely measured population.

And fifth, the small sample size effects are clearly evident when comparing the difference between the histogram and KDE estimates of the TDMI between Figs. 6(a) and 6(b). In particular, the two different estimates for the aggregate TDMI on $D_7$ are essentially identical, while the aggregated TDMI estimates on $D_8$ differ in a nontrivial way (by more than a factor of two). The average TDMI calculations display an even stronger effect. Finally, the error bars for $D_8$ are about ten times the magnitude of the error bars for $D_7$.

The point is, the time evolution of the TDMI is both scientifically valuable in that it leads to insights not otherwise observed and interpretable in the context of a time dependent, complex, diversely measured population using the infrastructure presented in this paper.

### *6. Independent analysis of the population composition of $D_7$ and $D_8$*

Based on the time-based information theoretic analysis we have reached the following population-composition hypotheses: data set seven represents a homogeneous population for $\delta t > 6hrs$ and is heterogeneous for $\delta t \leq 6hrs$; the subpopulation of data set eight used to estimate $\hat{I}(\delta t \leq 48)$ is relatively homogeneous, but less homogeneous than data set seven; overall, data set 8 is heterogeneous. However, because these populations are

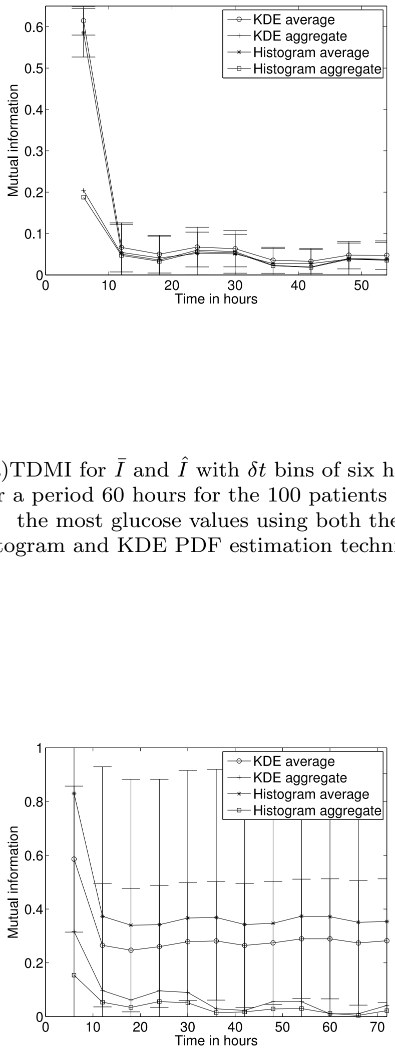

(a)TDMI for $\bar{I}$ and $\hat{I}$ with $\delta t$ bins of six hours for a period 60 hours for the 100 patients with the most glucose values using both the histogram and KDE PDF estimation techniques.

(b)TDMI for $\bar{I}$ and $\hat{I}$ with $\delta t$ bins of six hours for a period 72 hours for the $20,000$ randomly selected patients using both the histogram and KDE PDF estimation techniques.

FIG. 6: The TDMI for both $\bar{I}$ and $\hat{I}$ with $\delta t$ bins of six hours for a period of a few days. With respect to Fig. 6(a) note the following: for $\delta t \leq 6hrs$, $\delta I > 0$; for $\delta t > 6hrs$, $\delta I \approx 0$; the KDE and histogram estimates are extremely similar; the diurnal (daily) periodic variation in correlation of glucose is clearly evident in both $\bar{I}$ and $\hat{I}$. With respect to Fig. 6(b) note the following: for all $\delta t$ $\delta I$ is consistent and likely zero within bias; the KDE and histogram estimates differ greatly, implying the presence of small sample size effects in the average TDMI calculation; the diurnal (daily) periodic variation in correlation of glucose is clearly evident in both $\bar{I}$ and $\hat{I}$ in all but the KDE estimated TDMI average.

real patients from a hospital, we can also examine other sources of information regarding the qualitative types these populations represent. Specifically, we can consider the billing codes, which can act as a proxy for population composition, assigned to the patients in the various populations. It is important to note that the billing codes are *largely independent of the specific lab values*, and thus, can be seen as an outside test of the validity of the TDMI analysis.

We consider the fraction of patients with the two most frequent billing codes for three data sets, $D_7$, $D_8$, and the subset of $D_8$ used to estimate the TDMI-based diagnostics, $D_8'$ (members of the $D_8'$ subpopulation have at least 10 glucose measurements separated by six hours or less). Note that a patient is counted for having an billing code if it occurs only once. There are two features of that are important to pay attention to: (i) the overall fraction of patients that have a given billing code, and (ii), the drop off between the fraction of patients with the most and second most common billing codes. For $D_7$, 75% of the patients are covered by a single billing code and the drop between the most and second most common billing codes is around 5% — thus 70+% of these patients likely have relatively similar afflictions. In contrast, the most frequently seen billing code in $D_8$ only covers 25% of the population, followed by a 10 point drop off. In constrast, at least 50% of $D_8'$ is covered by a single billing code, while the second most common billing code only covers only a quarter of the population — a 25 point drop. This implies more homogeneity than $D_8$ but less than $D_7$. Broadly speaking, the billing code analysis corroborates the conclusions drawn from the time-based information theoretic analysis in the previous section. Nevertheless, the billing code analysis, being static, does not reveal the heterogeneity observed in $D_7$ at $\delta t = 6hrs$.

## X. SUMMARY

**Note, a explicit prescription for interpreting $I$ for a fixed time separation $\delta t$ for a population can be found in Fig. 2 within section VIII**. Moreover, an algorithmic portrayal can be found in appendix A 3.

**Results of the interpretative framework relative to real data.** The methods in this paper were shown to work for both a well understood computer-generated data set and for a pathologically diverse real data set. Thus, given a population of time-series that are: nonuniformly measured in time, of diverse lengths, from statistically diverse sources, nonstationary, and pathologically sparse, our methods will likely still yield interpretable results. The entropy for all populations registered the populations as diverse. Nevertheless, the TDMI produced a more nuanced picture. In particular, for one set of patients, the TDMI calculation implied that a set of patients have differing predictive information up to 6 hours, and are homogeneous in correlation afterwards. In contrast, the same calculation on a heavily filtered general population (the population that had frequent data measurements), yielded a population that seemed homogeneous with respect to time-dependent correlation. While these two sets of patients, according to their billing codes were similar, they differed in some key features. Thus, while it is likely that these populations are different, a full explanation, which requires more clinical study, is beyond the scope of this paper. Nevertheless, the TDMI analysis yielded results that were understandable, given this pathologically difficult population of data.

**How our method addresses nonstationarity.** At various points in this paper we have alluded to how nonstationarity is addressed within our framework. To be more explicit, consider three cases: (i) a single nonstationary source, (ii) multiple different stationary sources, and (iii) multiple different nonstationary sources. Relative to case (i), because there is no real sense of population average, $\delta I \approx 0$, $\hat{B}_{IRP} = \hat{B}_{PRP}$ and $\mathcal{H}_S \approx B_E$ — thus there will be no distinction between stationarity and nonstationarity. Case (ii) is the case we handled in section IX A and does not need explanation. And case (iii) will behave identically to case (ii); nonstationary will be difficult to detect, but multiple different statistical states will be detectable. While it might be too much to ask to be able to distinguish nonstationarity amongst a population from a population with multiple stationary sources, we can detect nonstationarity within an individual, given enough data points. In particular, relative to case (i), the reason why all the diagnostics fail to detect multiple statistical states is that there is *no concept of averaging over a population.* To address this issue, one only needs to partition the single time series into multiple pieces (of sufficient length), and then apply the standard TDMI analysis from this paper to the new "population" of time series. Said differently, the to detect nonstationarity in a single source, one only needs to treat the single source as multiple sources and apply our machinery; if it appears that there are multiple sources, then you know that the single source has multiple statistical states, and is thus nonstationary.

**Comments regarding the connection between the supports and the normalizations of the distributions.** In a sense, all support-based variation amongst the population could be eliminated by normalizing all individuals to some standard support (or to a distribution with mean zero and variance one). We did not implement this because sometimes the normalization of the support matters with respect to the composition of the population, and we wanted to allow for the TDMI infrastructure to capture this type of dependence. Relative to the example in this paper, having glucose oscillate around 500 means the patient is very sick, whereas glucose oscillation around 100 means the patient is likely healthy (at least from a blood glucose perspective) — we wanted to be able to capture this type of heterogeneity. That said, if one begins with a *normalized population* and performs the TDMI analysis, any $\delta I$ *must* exist because of variation in the *graphs* of the PDFs. However, if one has enough points per patient to estimate $\bar{I}$, one knows this anyway upon calculating $\hat{B}_{IRP}$ and $\hat{B}_{PRP}$; when there are not enough points to estimate $I$ for every individual, then deducing temporal, graph-based variation is difficult.

**Future directions regarding the use of this technique.** One of the sources of motivation for performing this calculation is based on the idea of stratifying or clustering populations of individuals by their predictive information. Based on the TDMI infrastructure here, we have identified at least 3 different subpopulations based on their predictive information structure. Thus future computational problems will involve developing and testing a more automated form of this interpretive structure that can be used for generating hypothesized sub-categories of individuals and eventually an infrastructure that can be integrated with classification and clustering schemes.

**Some remaining statistical problems.** In this work we attempted to outline and show, mathematically, how to interpret the TDMI and information entropy for aggregated populations. Nevertheless, there are many details that are remain. In particular, a partial list might include full rigorous proofs regarding: the technical conditions under which our claims (i.e., $\delta I > 0$ if an only if $\epsilon_i > 0$ for some $i$) apply; the convergence properties of various quantities we propose (i.e., $\delta I$, $\mathcal{H}_S$. etc); and the full relationships between what the information entropy and TDMI can imply about one another. The goal of this work was to propose a practically workable framework calculating the TDMI for complex populations of time series. However, this work leaves many interesting, more abstract questions remaining.

## XI. ACKNOWLEDGMENTS

The authors would like to thank J. Dias, N. Elhadad, A. Perotte, and D. Varn for carefully reading this paper and providing many useful comments. DJA would like to thank C. Shalizi for early discussions related to this work. Finally, the authors would like to acknowledge the financial support provided by NLM grant RO1 LM06910.

## Appendix A: Analysis of aggregation order

### 1. Detailed average TDMI calculation

Begin by recalling the definition of the average TDMI:

$$\bar{I}(\tau) = \frac{1}{N}\sum_{i=1}^{N}\int p(X_i(j), X_i(j-\tau)) \tag{A1}$$

$$\log(\frac{p(X_i(j), X_i(j-\tau))}{p(X_i(j))p(X_i(j-\tau))})dX_i(t)dX_i(t+\tau)$$

$$= \int \bar{\iota}(\tau)dX(t)dX(t+\tau).$$

Next, recall that for the average TDMI, we have PDFs defined entirely with respect to the abstract support, $\bar{\mathcal{S}}$. In this situation, we define the $i^{th}$ PDF relative to the "average" PDF, $p_1$, by:

$$p_i = p_1(\bar{\mathcal{S}}) - \bar{\epsilon}_i(\bar{\mathcal{S}}) \tag{A2}$$

where $\bar{\epsilon}_i(\bar{\mathcal{S}})$ is distance between the *graphs* of $p_1$ and $p_i$ at a given value in $\bar{\mathcal{S}}$. Next, for convenience, define the following: $p(X_i(j), X_i(j-\tau)) = p(j,\tau)$, $p(X_i(j)) = p(j)$, $p(X_i(j-\tau)) = p(\tau)$, $\bar{\epsilon}_i(\bar{\mathcal{S}}) = \bar{\epsilon}_i$, $p_i(j,\tau) = p_1(j,\tau) - \bar{\epsilon}_i$, $p_i(j) = p_1(j) - \bar{\epsilon}_i$, and $p_i(\tau) = p_1(\tau) - \bar{\epsilon}_i$. With this notation, we can now re-write *the integrand* in Eq. A1

$$= \frac{1}{N}[p_1(j,\tau)\log(\frac{p_1(j,\tau)}{p_1(j)p_1(\tau)}) + \tag{A3}$$

$$\sum_{i=2}^{N}(p_1(j,\tau) - \bar{\epsilon}_i)\log(\frac{p_1(j,\tau) - \bar{\epsilon}_i}{(p_1(j) - \bar{\epsilon}_i)(p_1(\tau) - \bar{\epsilon}_i)})] \tag{A4}$$

Next, factoring $\frac{p_1(j,\tau)}{p_1(j)p_1(\tau)}$ out of the summation term, one arrives at:

$$= \frac{1}{N}[p_1(j,\tau)\log(\frac{p_1(j,\tau)}{p_1(j)p_1(\tau)}) + \tag{A5}$$

$$\sum_{i=2}^{N}(p_1(j,\tau) - \bar{\epsilon}_i)[\log(\frac{p_1(j,\tau)}{(p_1(j))(p_1(\tau))}) + \tag{A6}$$

$$\log(\frac{1 - \frac{\bar{\epsilon}_i}{p_1(j,\tau)}}{1 - \frac{\bar{\epsilon}_i}{p_1(j)p_1(\tau)}(p_1(j) + p_1(\tau)) + \frac{\bar{\epsilon}_i^2}{p_1(j)p_1(\tau)}})]]. \tag{A7}$$

Multiplying and collecting terms under the sum, one obtains:

$$= \frac{1}{N}[Np_1(j,\tau)\log(\frac{p_1(j,\tau)}{p_1(j)p_1(\tau)}) + \tag{A8}$$

$$\sum_{i=2}^{N}\bar{\epsilon}_i[\log(\frac{p_1(j,\tau)}{(p_1(j))(p_1(\tau))}) + \tag{A9}$$

$$\log(\frac{1 - \frac{\bar{\epsilon}_i}{p_1(j,\tau)}}{1 - \frac{\bar{\epsilon}_i}{p_1(j)p_1(\tau)}(p_1(j) + p_1(\tau)) + \frac{\bar{\epsilon}_i^2}{p_1(j)p_1(\tau)}})] + \tag{A10}$$

$$p_1(j,\tau)\log(\frac{1 - \frac{\bar{\epsilon}_i}{p_1(j,\tau)}}{1 - \frac{\bar{\epsilon}_i}{p_1(j)p_1(\tau)}(p_1(j) + p_1(\tau)) + \frac{\bar{\epsilon}_i^2}{p_1(j)p_1(\tau)}})] \tag{A11}$$

$$= \bar{\rho}(\tau) + \frac{1}{N}[\sum_{i=2}^{N}\bar{\epsilon}_i[\log(\frac{p_1(j,\tau)}{(p_1(j))(p_1(\tau))}) + \tag{A12}$$

$$\log(\frac{1 - \frac{\bar{\epsilon}_i}{p_1(j,\tau)}}{1 - \frac{\bar{\epsilon}_i}{p_1(j)p_1(\tau)}(p_1(j) + p_1(\tau)) + \frac{\bar{\epsilon}_i^2}{p_1(j)p_1(\tau)}})] + \tag{A13}$$

$$p_1(j,\tau)\log(\frac{1 - \frac{\bar{\epsilon}_i}{p_1(j,\tau)}}{1 - \frac{\bar{\epsilon}_i}{p_1(j)p_1(\tau)}(p_1(j) + p_1(\tau)) + \frac{\bar{\epsilon}_i^2}{p_1(j)p_1(\tau)}})] \tag{A14}$$

$$= \bar{\rho}(\tau) + \bar{G}(\tau) \tag{A15}$$

where $\bar{G}(\tau)$ can be shown to have the more digestible form:

$$\begin{aligned}\bar{G}(\tau) = &\\ &- \frac{1}{N}[\sum_{i=1}^{N-1}\left(\frac{\bar{\epsilon}_i}{p(X_1(j), X_1(j-\tau))}\right)\\ &\left(\log\frac{p(X_1(j), X_1(j-\tau))}{p(X_1(j))p(X_1(j-\tau))}\right)\\ &+ \log\left(\frac{1 - \frac{\bar{\epsilon}_i}{p(X_1(j),X_1(j-\tau))}}{(1 - \frac{\bar{\epsilon}_i}{p(X_1(j))})(1 - \frac{\bar{\epsilon}_i}{p(X_1(j-\tau))})}\right)\\ &\left(\frac{\bar{\epsilon}_i}{p(X_1(j), X_1(j-\tau))} - 1\right)]\end{aligned} \tag{A16}$$

### 2. Detailed aggregate TDMI calculation

Begin by recalling the definition of the TDMI for an aggregate population:

$$\hat{I}(\tau) = \int p(X_1^{n-\tau}; X_\tau^n)\log(\frac{p(X_1^{n-\tau}; X_\tau^n)}{p(X_1^{n-\tau})p(X_\tau^n)})dX_1^{n-\tau}dX_\tau^n \tag{A17}$$

$$= \int \hat{\imath}(\tau)dX_1^{n-\tau}dX_\tau^n$$

Next, recall that in this situation we first select an "average" PDF relative to the abstract support $\hat{\mathcal{S}}$ and then we define the $i^{th}$ PDF relative to this "average" PDF on the *total support* $\hat{S}$, $p_1$, by:

$$p_i = p_1(\hat{S}) - \hat{\epsilon}_i(\hat{S}) \tag{A18}$$

where $\hat{\epsilon}_i(\hat{S})$ is distance between the *graphs* of $p_1$ and $p_i$ at a given value in $\hat{S}$. Next, for convenience, define the following: $p(X_i(j), X_i(j-\tau)) = p_i(j,\tau)$, $p(X_i(j)) = p_i(j)$, $p(X_i(j-\tau)) = p_i(\tau)$, $\hat{\epsilon}_i(\hat{S}) = \hat{\epsilon}_i$, $p_i(j,\tau) = p_1(j,\tau) - \hat{\epsilon}_i$, $p_i(j) = p_1(j) - \hat{\epsilon}_i$, and $p_i(\tau) = p_1(\tau) - \hat{\epsilon}_i$, never forgetting that all of these quantities depend on a particular value in the support, $\hat{S}$. With this notation, we can now re-write *the integrand* in Eq. A17 in terms of only $p_1$ and $\hat{\epsilon}$, arriving at:

$$= \frac{1}{N}\sum_{i=1}^{N}(p_1(j,\tau) - \hat{\epsilon}_i) \tag{A19}$$

$$(\log(\frac{\frac{1}{N}\sum_{i=1}^{N}(p_1(j,\tau) - \hat{\epsilon}_i)}{(\frac{1}{N}\sum_{i=1}^{N}(p_1(j) - \hat{\epsilon}_1))(\frac{1}{N}\sum_{i=1}^{N}(p_1(\tau) - \hat{\epsilon}_1))})) \tag{A20}$$

Next, factoring $p_1(j,\tau)$, $p_1(j)$, and $p_1(\tau)$ out of the numerator of the summation terms, one arrives at:

$$=(\frac{p_1(j,\tau)}{N}\sum_{i=1}^{N}(1-\frac{\hat{\epsilon}_i}{p_1(j,\tau)})) \tag{A21}$$

$$\log(\frac{\frac{p_1(j,\tau)}{N}\sum_{i=1}^{N}(1-\frac{\hat{\epsilon}_i}{p_1(j,\tau)})}{(\frac{p_1(j)}{N}\sum_{i=1}^{N}(1-\frac{\hat{\epsilon}_i}{p_1(j)}))(\frac{p_1(\tau)}{N}\sum_{i=1}^{N}(1-\frac{\hat{\epsilon}_i}{p_1(\tau)})))} \tag{A22}$$

which, after collecting terms, becomes:

$$\hat{\iota} =(p_1(j,\tau)-\sum_{i=1}^{N}\frac{\hat{\epsilon}}{Np_1(j,\tau)}) \tag{A23}$$

$$(\log(\frac{p_1(j,\tau)}{p_1(j)p_1(\tau)})+\log\frac{1-\sum_{i=1}^{N}\frac{\hat{\epsilon}_i}{Np_1(j,\tau)}}{(1-\sum_{i=1}^{N}\frac{\hat{\epsilon}_i}{Np_1(j)})(1-\sum_{i=1}^{N}\frac{\hat{\epsilon}_i}{Np_1(\tau)})}). \tag{A24}$$

Next, collecting the $p_1(j,\tau)\log(\frac{p_1(j,\tau)}{p_1(j)p_1(\tau)})$ term, one gets:

$$\hat{\iota} = p_1(j,\tau)\log(\frac{p_1(j,\tau)}{p_1(j)p(\tau)})+\hat{G}(\tau) \tag{A25}$$

where $\hat{G}$ is given by:

$$\hat{G}(\tau) =\log\left(\frac{1-\frac{\sum_{i=1}^{N-1}\hat{\epsilon}_i}{Np_1(j,\tau)}}{(1-\frac{\sum_{i=1}^{N-1}\hat{\epsilon}_i}{Np_1(j)})(1-\frac{\sum_{i=1}^{N-1}\hat{\epsilon}_i}{Np_1(\tau)})}\right)$$
$$\left(p_1(j,\tau)-\frac{\sum_{i=1}^{N-1}\hat{\epsilon}_i}{N}\right) \tag{A26}$$
$$-\frac{\sum_{i-1}^{N-1}\hat{\epsilon}_i}{N}\log\left(\frac{p_1(j,\tau)}{p_1(j)p_1(\tau)}\right)$$

### 3. Pseudocode for interpreting the TDMI for a population of time series

[1] C. Komalapriya, M. Thiel, M. C. Ramano, N. Marwan, U. Schwarz, and J. Kurths. Reconstruction of a system's dynamics from short trajectories. *Phys. Rev. E.*, 78:066217, 2008.

[2] J. C. Sprott. *Chaos and Time-series Analysis.* Oxford University Press, 2003.

[3] H. Kantz and T. Schreiber. *Nonlinear Time Series Analysis.* Cambridge University Press, $2^{nd}$ edition, 2003.

[4] W. Hogan and M. Wagner. Accuracy of data in computer-based patient records. *J. Am. Med. Inform. Assoc.*, 5:342, 1997.

[5] J. van der Lei. Use and abuse of computer stored medical records. *Meth. Inform. Med.*, 30:79, 1991.

[6] H. Sagreiya and R. B. Altman. The utility of general perpose versus specialty clinical databased for research: Warfarin dose estimation form extracted clinical variables. *J. Bio. Info.*, 43:747–751, 2010.

[7] JM Higgins and L Mahadevan. Physiological and pathological population dynamics of circulating human red blood cells. *PNAS*, 107:20587–20592, 2010.

[8] E. Shudo, R. M. Ribeiro, and A. S. Perelson. Modelling hepatitis c virus kinetics during treatment with pegylated interferon $\alpha-2\beta$: errors in the estimation of viral kinetic parameters. *J Viral Hepat.*, 15:357–362, 2008.

[9] M. S. Turner. A century of physics: 1950-2050. *Physics Today*, 62:8–9, 2009.

[10] J. D. Scargle. Studies in astronomical time series analysis ii Statistical aspects of spectral analysis of unevenly spaced data. *Astrophys. J.*, 263:835–853, 1982.

[11] S. Baisch and G. H. R. Bokelmann. Spectral analysis with incomplete time series: An example form seismology. *Comput. Geosci.*, 25:739–750, 1999.

[12] M. Schulta and K. Stattegger. Spectrum: Spectral analysis of unevenly spaced paleoclimatic time series. *Comput. Geosci.*, 23:929–945, 1997.

[13] A. W. C. Liew, J. Xian, S. Wu, D. Smith, and H. Yan. Spectral estimation in unevenly sampled space of periodically expressed microarray time series data. *BMC Bioinformatics*, 8:137–156, 2007.

[14] L. Wasserman. *All of Statistics: A Concise Course in Statistical Inference.* Springer, 2004.

[15] Loéve. *Probability Theory I.* Springer-Verlag, 1977.

[16] Gray and Moore. Very fast multivariate kernel density estimation using via computational geometry. In *Joint Stat. Meeting*, 2003.

[17] Y-I Moon, B. Rajagopalan, and U. Lall. Estimation of mutual information using kernel density estimators. *Phys. Rev. E*, 52:2318 – 2321, 1995.

[18] R. J. May, G. C. Dandy, H. R. Maier, and T.M.K. Gayani Fernando. Critical values of a kernel density-based mutual information estimator. In *International Joint Conference on Neural Networks.* IEEE, 2006.

[19] D. J. Albers and G. Hripcsak. Estimation of time-delayed mutual information from sparsely sampled sources. Submitted, 2011.

[20] Richard L. Wheeden and Antoni Zygmund. *Measure and integral*, volume 43 of *Monographs and textbooks in pure and applied mathematics.* Marcel Dekker, Inc., 1977.

[21] G. P. Basharin. On a statistical estimate for entropy of a sequences of independent random variables. *Theory Prop. App.*, 4:333–338, 1959.

[22] M. S. Roulston. Estimating the errors on measured entropy and mutual information. *Physica D*, 125:285–294, 1999.

**Algorithm 1** How to interpret the TDMI for a population of time series

```
if there are enough points to estimate $\bar{I}$ (usually $\sim 100$ pairs of points per representative individual are required) then
    estimate $\delta I$ and $H_\Theta$
    if $\delta I > B_{IRP}$ then
        the population is heterogeneous
        if $\mathcal{H}_S \sim 0$ then
            supports (or ranges) are diverse or disjoint
        else if $\mathcal{H}_S \sim 1$ then
            supports (or ranges) are uniform
        end if
    else if $\delta I \leq B_{IRP}$ then
        the population is homogeneous
    end if
    if $H_\Theta \sim 0$ then
        the population is well represented
    else if $H_\Theta \sim 1$ then
        the portions of the population are overrepresented
    end if
else if not enough pairs to estimate $\bar{I}$ then
    estimate $\hat{I}$, $\mathcal{H}_S$, and $H_\Theta$
    if $\mathcal{H}_S \sim 0$ then
        supports (or ranges) are diverse or disjoint
        if there are enough pairs of points per patient to estimate a PDF for each patient at the specific $\delta t$ then
            $V_{\hat{S}}(p)$ (i.e., $V(p)$ relative to the abstract supports)
            if $V_{\hat{S}}(p) \sim 1$ then
                the population used to estimate $\hat{I}$ has graph-based heterogeneity
            else if $V_{\hat{S}}(p) \sim 0$ then
                the population used to estimate $\hat{I}$ is graphically homogeneous
            end if
        else if it is not possible to accurately estimate a PDF for each patient at the specific $\delta t$ then
            it is not possible to determine the contribution of the graph-based heterogeneity to the overall heterogeneity
        end if
    else if $\mathcal{H}_S \sim 1$ then
        supports (or ranges) are uniform
        if $V_{\bar{S}}(p) \sim 1$ then
            the population used to estimate $\hat{I}$ has graph-based heterogeneity
        else if $V_{\bar{S}}(p) \sim 0$ then
            the population used to estimate $\hat{I}$ is homogeneous
        end if
    end if
    if $H_\Theta \sim 0$ then
        the population is well represented
    else if $H_\Theta \sim 1$ then
        the portions of the population are overrepresented
    end if
end if
{NOTE: there are 10 possible sharp interpretations for both $\delta I$ and $\hat{I}$-only cases.}
{All TDMI interpretations should include: $I$-like quantities (e.g., $\hat{I}$, $\delta I$, etc), population diversity qualification (support- and graph-based contributions to diversity; if they are unknown, this should be specified), and the make-up of the population used to estimate the $I$-based quantities (e.g., $H_\Theta$.}
{NOTE: even under the best circumstances, it may be difficult to determine what proportion of the heterogeneity is due to support-based versus graph-based diversity.}
```

[23] J. Graxzyk and G. Światek. Generic hyperbolicity in the logistic family. *Ann. of Math.*, 146:1–52, 1997.

[24] M. Jakobson. Absolutely continuous invariant measures for one-parameter families of one-dimensional maps. *Commun. Math. Phys.*, 81:39–88, 1981.

[25] D. J. Albers and G. Hripcsak. A statistical dynamics approach to the study of human health data: resolving population scale diurnal variation in laboratory data. *Physics Lett. A*, 2010.

[26] D. J. Albers and G. Hripcsak. Using population scale (ehr) data to understand and test human physiological dynamics. submitted.

[27] It may seem odd to normalize indices, but this just keeps the domain of $\tilde{\Theta}$ between zero and one.

[28] To see the variation in the PDF estimates due to small sample sizes, observe the PDF estimates for different sets of uniform random numbers with small cardinality.

[29] Note, the $L_1$ difference is not technically a distance function or a metric because it does not satisfy the triangle inequality.